Editorial

〔Lab Med Int 2025; 4(1): 1-2〕

New findings on hypertriglyceridemia during pregnancy

*Takeyoshi Murano, PhD**

* Clinical Laboratory Program, Faculty of Science, Toho University, Funabashi-shi, Chiba, 274-8510, Japan.
E-mail: murano@sci.toho-u.ac.jp

See article volume 4(1): 29-33

Severe hypertriglyceridemia, characterized by extremely high levels of triglycerides in the blood, is a significant risk factor for the development of acute pancreatitis, a severe and potentially life-threatening condition [1]. Acute pancreatitis occurs when the pancreas becomes inflamed, often leading to symptoms such as severe abdominal pain, nausea, vomiting, and, in some cases, systemic complications like organ failure. The presence of severe hypertriglyceridemia can exacerbate these effects by contributing to the formation of free fatty acids through the breakdown of triglycerides by pancreatic lipase. These free fatty acids can damage pancreatic cells and contribute to the inflammatory process. During pregnancy, the risk associated with severe hypertriglyceridemia is heightened due to physiological changes, such as increased insulin resistance and hormonal shifts, which can exacerbate lipid imbalances. When acute pancreatitis develops in this context, it can have catastrophic consequences, including preterm labor, severe maternal complications such as multi-organ failure, and even fetal loss or stillbirth [2]. Despite these severe outcomes, the precise mechanisms by which hypertriglyceridemia triggers acute pancreatitis-especially in pregnant women-remain poorly understood. Previous researches suggest that factors such as genetic predisposition, hormonal modulation of lipid metabolism, and inflammation might play crucial roles, but further investigation is required to clarify these pathways. This study by Sadakata and colleagues is elucidating the mechanism of abnormal lipid metabolism during pregnancy. The researchers investigated the involvement of glycosylphosphatidylinositol-anchored high-density lipoprotein-binding protein 1 (GPIHBP1), an anchor protein for lipoprotein lipase (LPL) – a key enzyme in lipid metabolism – by measuring its blood levels during different pregnancy stages. GPIHBP1 has recently attracted attention as a potential cause of severe hypertriglyceridemia. It plays a crucial role not only in the transport of LPL to the subendothelium of blood vessels but also in facilitating the binding of LPL to the surface of vascular endothelial cells, making it a vital component in LPL metabolism [3]. Cases of hyperchylomicronemia, thought to be caused by GPIHBP1 deficiency or GPIHBPI autoantibodies, have been reported [3,4]. In this study, during different pregnancy stages, blood concentrations of GPIHBP1 and LPL were observed to decrease transiently, returning to nonpregnant levels after delivery. When adjusted for albumin concentration, the decrease in GPIHBP1 levels was negated. However, LPL levels continued to show a transient decrease during late pregnancy, even after adjusting for albumin levels. These results suggest that during the course of normal pregnancy, the transient decrease in GPIHBP1 levels may be attributed to physiological dilution. In contrast, the transient decrease in blood LPL levels is likely due to inhibited lipolysis. This study has several limitations, including the reliability of the blood sample data and the influence of insulin resistance. To confirm these findings, further research is needed to elucidate the underlying mechanisms.

Refference

1) Yang AL, McNabb-Baltar J. Hypertriglyceridemia and acute pancreatitis. Pancreatology 2020; 20 (5) : 795-800. doi: 10.1016.

2) Gupta M, Liti B, Barrett C, et al. Prevention and Management of Hypertriglyceridemia-Induced Acute Pancreatitis During Pregnancy: A Systematic Review. Am J Med 2022; 135 (6) : 709-14.

3) Beigneux AP, Miyashita K, Ploug M, et al. Autoantibodies against GPIHBP1 as a Cause of Hypertriglyceridemia. N Engl J Med 2017; 376 (17) : 1647-58.

4) Rios JJ, Shastry S, Jasso J, et al. Deletion of GPIHBP1 causing severe chylomicronemia. J Inherit Metab Dis 2012; 35 (3): 531-40. doi: 10.1007/s10545-011-9406-5.

Case Report

Acute amebic appendicitis associated with relapsing amebic infection: a case report

†Ayumu Kurihara[*1,2], *Tadakazu Ao*[*3], *Hiroaki Takeo*[*1], *Susumu Matsukuma*[*2]

†Corresponding author: Ayumu Kurihara, E-mail: doc41029@ndmc.ac.jp
Received May 16, 2024; accepted September 6, 2024
*1 Department of Pathology, Japan Self-Defense Forces Central Hospital, Tokyo, Japan.
*2 Department of Pathology and Laboratory Medicine, National Defense Medical College, Saitama, Japan.
*3 Department of Surgery, Japan Self-Defense Forces Central Hospital, Tokyo, Japan.

ABSTRACT

Acute amebic appendicitis, a rare presentation of *Entamoeba histolytica* infection, is challenging to distinguish from non-amebic appendicitis because of similarities in symptoms and laboratory data. Here, we describe the case of a 42-year-old Japanese male with amebic appendicitis diagnosed by histopathological examination of the removed appendiceal specimens. In this case, blood eosinophilia was not observed, and amebic trophozoites were histologically distributed not only in surface exudates but also in appendiceal submucosa and muscularis propria. In addition, a thorough interview and additional colonoscopy after the diagnosis revealed a history of amebic colitis and persistent amebic colitis. We believe that physicians should be aware of the possible presence of amebic appendicitis because of its higher mortality rate compared to non-amebic appendicitis.

〔Lab Med Int 2025; 4(1): 3-7〕

Key Words
amebiasis, acute appendicitis, *Entamoeba histolytica*, amebic colitis, eosinophilia

I. Introduction

The main manifestations of *Entamoeba histolytica* (*E. histolytica*) infection are amebic colitis and amebic liver abscess.[1] Almost all (93%) cases of amebic colitis involve the ileocecal region;[2] however, amebic appendicitis is rare,[2] accounting for only 0.5–2.3% of acute appendicitis cases even in endemic developing countries.[3] Amebic appendicitis is frequently overlooked clinically, and its definite diagnosis requires pathological examination of the removed vermiform appendix, thus delaying therapy.[4),5] Here, we describe the unique clinicopathological findings of a pertinent case to expand our knowledge of amebic appendicitis.

II. Case report

A 42-year-old Japanese male was brought to our hospital by ambulance because of exacerbating and moving abdominal pain. The patient was an office worker, and had a history of depression. Physical examination revealed localized tenderness in the right lower abdomen, with muscle guarding. Laboratory tests of peripheral blood revealed a white blood cell (WBC) count of 12,080 /μL without eosinophilia (240 /μL) and serum C-reactive protein (CRP) level of 0.49 mg/dL. Serum albumin is 4.6 g/dL and other serological data ruled out human immunodeficiency virus, hepatitis B virus, and hepatitis C virus infection, so there was no evidence of malnutrition or immunodeficiency. Computed tomography revealed a thickened appendiceal wall with contrast enhancement, multiple appendicoliths, and periappendiceal fat stranding. These findings suggested acute appendicitis. Laparoscopy revealed minimal ascites and no peritoneal abscess, and appendectomy was performed. On post-operative day (POD) 3, serum CRP level was slightly elevated but WBC was decreased (2.46 mg/dL and 3,790 /μL, respectively), and on POD 4, the patient was discharged without any complication. On POD5, the

appendectomized specimen was pathologically diagnosed as an amebic infection. On POD18, an in-depth medical interview was performed and revealed the patient's hidden medical history: 1) one year before this episode, the patient had been diagnosed with amebic colitis of entire colon by colonoscopy at another clinic; 2) the patient was treated with 5-days oral metronidazole, his symptoms disappeared, and his follow-up at the clinic was completed. By POD18, serum CRP levels and WBC count were within normal ranges and his symptom was disappeared, so additional treatment seemed unnecessary, but we recommended colonoscopy just in case. On POD49, the patient underwent additional colonoscopy at the clinic, and biopsy specimens from the ileocecal erosive lesions showed a relapsing amebic infection without colitis of any other part. The patient was given a 10-day metronidazole treatment. Six months after treatment, a follow-up colonoscopy revealed complete endoscopic remission, and the patient is alive and well.

III. Histopathological Findings

The removed vermiform appendix showed dark mucosal changes at the tip (**Figure 1**). Microscopically, a neutrophil-predominant inflammatory infiltrate with a small number of eosinophils, lymphocytes, and plasma cells involved the entire thickness of the appendiceal wall, chiefly located on the appendiceal tip, accompanied by focal ulcers. Hematoxylin and eosin (HE) -stained sections identified oval amebic trophozoites with foamy cytoplasm and eosinophilic nucleus-like structures (**Figure 2**). These amebic trophozoites are highlighted in bright red by periodic acid-Schiff (PAS) staining (**Figure 2b**, inset). Amebic trophozoites were predominantly distributed within the appendiceal wall rather than on the surface (**Figure 3**). Trophozoites phagocytosed erythrocytes in the cytoplasm suggest active inflammation.

Figure 1 Macroscopic findings of removed appendix vermiformis. Dark colored mucosa was seen in the tip (left of the image).

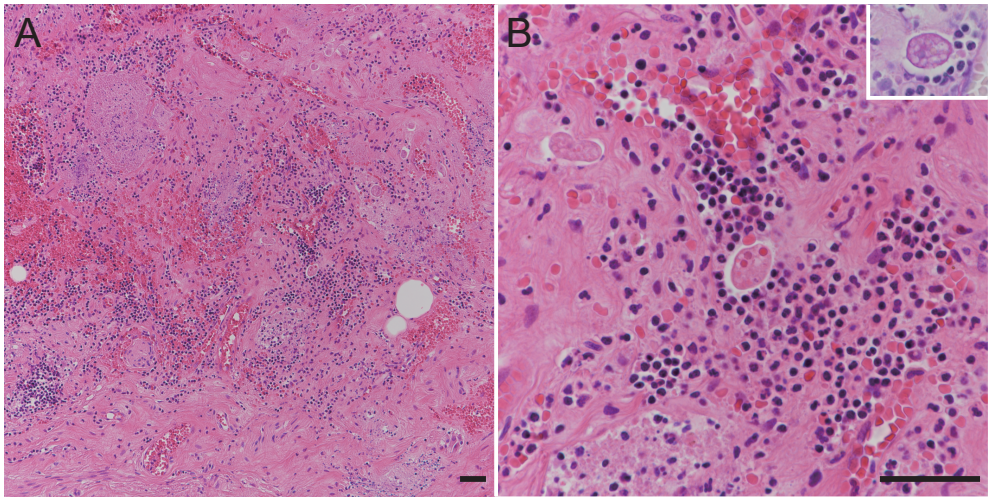

Figure 2 Histopathological features of amebic appendicitis.

A. Moderate-power view showing scattered amebic trophozoites within appendiceal submucosa.

B. High-power view of oval amebic trophozoites with foamy cytoplasm and eosinophilic nucleus-like structures. Periodic acid-Schiff stain highlighting reddish features of trophozoite (inset) (A, hematoxylin and eosin stain, ×100; B, hematoxylin and eosin stain, ×400; inset, periodic acid-Schiff stain, ×400, black bars, 50 μm).

IV. Discussion

E. histolytica infection, or amebiasis, is the second leading cause of death from parasitic infection worldwide.[6] In Japan, the annual incidence of amebiasis is low (approximately 500 cases per year) owing to a clean water supply,[7] and amebic appendicitis is extremely rare. Our review of Japanese literature revealed only 18 previous reports describing surgically treated amebic appendicitis.[5),8] There is a male preponderance in the Japanese incidence of amebic infections, including colitis, liver abscess, and appendicitis.[7] In Japan, amebiasis is typically found in men who have sex with men and in individuals with recent travel to endemic areas. However, the present case had no history of travel abroad, and the infectious route was unclear.

Amebic colitis is not uncommon and is usually suspected based on clinical symptoms of bloody and/or mucous diarrhea and is diagnosed by colonoscopic, serological, or stool examination.[1] However, amebic appendicitis usually does not show bloody and/or mucous stools suggestive of amebic colitis, although appendicitis sometimes accompanies ileocecal amebic colitis.[3),4] The clinical symptoms of previously reported cases of amebic appendicitis and the present case were similar to those of non-amebic appendicitis, including right lower quadrant pain, fever, abdominal tenderness, and guarding. Therefore, the preoperative suspicion of amebic infection is considered difficult. Furthermore, in the present case, blood eosinophilia was not observed despite parasitic infection. Our review of the literature revealed four previous articles on amebic colitis or appendicitis describing the presence or absence of eosinophilia (**Table 1**). Three of these articles described three cases of amebic colitis without blood eosinophilia.[9)-11] The other article investigated amebic appendicitis in the pediatric population and revealed blood eosinophilia in only 14.2% of cases.[12] Therefore, blood eosinophilia is not always observed in patients with amebic appendicitis or colitis.

Previous systematic reviews of worldwide amebic appendicitis showed a mortality rate of 3.3%,[3] higher than that of overall acute appendicitis (0.09–0.24%),[13] although almost half of the cases included in this review were from endemic countries where metronidazole (medication for amebiasis) is routinely administered to all cases of acute appendicitis.[14] The mortality rate of amebic appendicitis is reported to be higher in Japan (25%).[5] This higher mortality rate would be attributed not only to post-operative complications such as amebic pancolitis, colonic perforation, peritonitis but also to delay for specific treatments.[4),8] Discrimination between amebic and non-specific appendicitis should be required.

The diagnosis of amebic appendicitis may be challenging not only clinically but also pathologically. In previous cas-

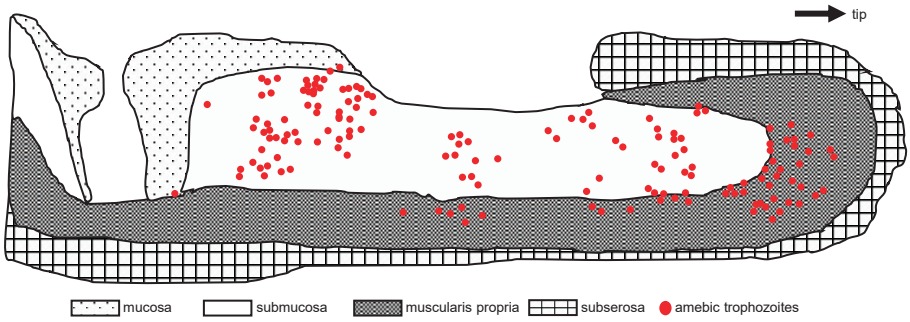

Figure 3 Schematic distribution of amebic trophozoites within longitudinal section of the vermiform appendix. Amebic trophozoites predominantly involving the submucosa and muscularis propria, rather than appendiceal surface.

Table 1 Relationship between blood eosinophilia and intestinal amebiasis.

Study	No of patients.	Age (years), Sex	Final Diagnosis	Blood eosinophilia
Shijubou et al[9]	1	68, M	Fulminant amebic colitis	None (count 160/μL)
Ohnishi et al[10]	1	30, M	Amebic colitis	None (count 162/μL)
Yasumura et al[11]	1	50, M	Fulminant amebic colitis	None (count 172/μL)
Escobar et al[12]	23	Mean 9 (3–15); M, 12; F, 11	AA (11), IA (12)	14.2%* of all cases (AA and IA)
Present case	1	42, M	AA	None (count 240/μL)

M, male; F, female; AA, amebic appendicitis; IA, acute appendicitis with incidental amebiasis (amebae found only within the appendiceal lumen)
* The total number of cases showing blood eosinophilia was not available from the article.

es,[4),5)] the first pathological examination of appendectomized specimens failed to reveal amoebas, and pathological reexamination based on clinical indications led to the accurate diagnosis of amebic appendicitis. In the present case, the amebic trophozoites involved not only the surface but also the appendiceal wall. Similar amebic distribution has been reported previously [15),16)] and seemed to differ from the surface-predominant lesions of amebic colitis.[17)] The appendiceal muscularis propria is rich in ganglion cells that mimic amebic trophozoites, which may contribute to their being overlooked at first glance. Furthermore, one pediatric study of amebic appendicitis reported higher perforation rate in wall involvement cases than in luminal colonization cases.[12)] Therefore, pathologists should be aware of the characteristic features of amebic appendicitis.

In amebic appendicitis, early metronidazole treatment lowers the mortality rate.[3)] Paromomycin, after metronidazole, is recommended to eliminate intestinal colonization.[1)] In the present case, an amebic infection predominantly involving the deep appendiceal wall may have been related to resistance to metronidazole treatment and relapse.

V. Conclusion

This case report describes an unusual case of acute appendicitis. In this case, eosinophilia was not observed, and *E. histolytica* trophozoites, highlighted by PAS staining, diffusely involved the removed vermiform appendiceal wall. Physicians should be aware of the presence of amebic appendicitis mimicking non-amebic appendicitis.

Author contribution

Kurihara A contributed to research and writing. Tadakazu A contributed to the editing of clinical findings. Takeo H and Matsukuma S contributed to the editing of pathological and laboratory findings.

Conflict of interest: The authors declare no conflicts of interest.

Funding: None.

Acknowledgements: We would like to thank Editage (www.editage.jp) for English language editing.

References

1) Haque R, Huston CD, Hughes M, et al. Amebiasis. N Engl J Med 2003; 348 (16): 1565-73. doi: 10.1056/NEJMra0227102.
2) Horiki N, Furukawa K, Kitade T, et al. Endoscopic findings and lesion distribution in amebic colitis. J Infect Chemother. 2015; 21 (6): 444-8. doi: 10.1016/j.jiac.2015.02.004.
3) Otan E, Akbulut S, Kayaalp C. Amebic acute appendicitis: systematic review of 174 cases. World J Surg 2013; 37 (9): 2061-73. doi: 10.1007/s00268-013-2079-5.
4) Suzuki Y, Adachi Y, Yasumizu R, et al. [Amebiases: Two autopsy cases where diagnosis could not be established during the lifetime of the patients] Seizen ni shindan no konnan de atta sekiri ameba kansensyo no 2 boukenrei. Jpn J Diagn Pathol. 2005; 22 (1): 25-8 (in Japanese).
5) Ito D, Hata S, Shimizu S, et al. Amebiasis presenting as acute appendicitis: Report of a case and review of Japanese literature. Int J Surg Case Rep 2014; 5 (12): 1054-7. doi: 10.1016/j.ijscr.2014.10.035.
6) Kantor M, Abrantes A, Estevez A, et al. Entamoeba histolytica: Updates in clinical manifestation, pathogenesis, and vaccine development. Can J Gastroenterol Hepatol 2018; 2018: 4601420. doi: 10.1155/2018/4601420.
7) Ishikane M, Arima Y, Kanayama A, et al. Epidemiology of domestically acquired amebiasis in Japan, 2000 – 2013. Am J Trop Med Hyg 2016; 94 (5): 1008-14. doi: 10.4269/ajtmh.15-0560.
8) Sugiyama Y, Osaka Y, Kato F, et al. A case of amebic appendicitis with abdominal wall necrosis, intestinal perforation, and infectious myocarditis after surgery. J Jpn Surg Assoc. 2021; 82 (8): 1537-42. doi: 10.3919/jjsa.82.1537 (in Japanese).
9) Shijubou N, Sumi T, Kamada K, et al. Fulminant amebic colitis in a patient with concomitant cytomegalovirus infection after systemic steroid therapy: A case report. World J Clin Cases 2021; 9 (15): 3726-32. doi: 10.12998/wjcc.v9.i15.3726.
10) Ohnishi K, Murata M, Okuzawa E. Symptomatic amebic colitis in a Japanese homosexual AIDS patient. Intern Med 1994; 33 (2): 120-2. doi: 10.2169/internalmedicine.33.120.
11) Yasumura K, Aoyama I, Shibata K, et al. [Early endoscopic diagnosis can save lives and reduce the extent of colon resection for acute fulminant amebic colitis: a case report with review]. Nihon Shokakibyo Gakkai Zasshi. 2022; 119 (6): 540-50. doi: 10.11405/nisshoshi.119.540 (in Japanese).
12) Echeverry JME, Valero JJ, Jaramillo LE, et al. Clinical features of amoebic appendicitis in children: A study of 23 cases. J Pediatr Surg 2021; 56 (8): 1362-4. doi: 10.1016/j.jpedsurg.2020.12.027.
13) Bhangu A, Søreide K, Saverio SD, et al. Acute appendicitis: modern understanding of pathogenesis, diagnosis, and management. Lancet 2015; 386 (10000): 1278-87. doi: 10.1016/S0140-6736 (15) 00275-5.
14) Guzmán-Valdivia G. Acute amebic appendicitis. World J Surg 2006; 30 (6): 1038-42. doi: 10.1007/s00268-005-0104-z.
15) Goyal A, Goyal S, Gupta CR. Acute amoebic appendicitis: An unusual presentation of a usual infection. Indian J

Pathol Microbiol. 2019; 62 (1) : 169-70. doi: 10.4103/IJPM.IJPM_576_17.

16) Kleitsch WP, Kisner P. Amebic appendicitis, peritonitis and wound infection. Ann Surg 1951; 133 (1) : 139-42. doi: 10.1097/00000658-195101000-00017.

17) Yue B, Meng Y, Zhou Y, et al. Characteristics of endoscopic and pathological findings of amebic colitis. BMC Gastroenterol. 2021; 21 (1) : 367. doi: 10.1186/s12876-021-01941-z.

Original

The utility of the enhanced liver fibrosis (ELF) score in Japanese patients with chronic hepatitis or cirrhosis

†Noriyuki Kuroda, PhD[1], Koji Fujita, MD, PhD*[2], Hitomi Imachi, MD, PhD*[1,3], Joji Tani, MD, PhD*[2], Asahiro Morishita, MD, PhD*[2], Kyoko Oura, MD, PhD*[2], Tomoko Tadokoro, MD, PhD*[2], Hideki Kobara, MD, PhD*[2], Koji Murao, MD, PhD*[1,3], Masafumi Ono, MD, PhD*[2], Tsutomu Masaki, MD, PhD*[2]*

†Correspondence: Division of Clinical Laboratory, Department of Medical Technology, Kagawa University Hospital, Ikenobe, 1750-1, Miki, Kita, Kagawa 761-0793, Japan.
E-mail: Kuroda.noriyuki. j5@ kagawa-u.ac.jp
Received March 25, 2024; accepted September 6, 2024
*[1] Division of Clinical Laboratory, Department of Medical Technology, Kagawa University Hospital
*[2] Department of Gastroenterology and Neurology, Faculty of Medicine, Kagawa University
*[3] Department of Endocrinology and Metabolism, Faculty of Medicine, Kagawa University

ABSTRACT

Objectives: The ELF scores, a non-invasive serum marker for liver fibrosis, has primarily been utilized in Western countries as an alternative to liver biopsy. In this study, we assessed its diagnostic efficacy in Japanese patients by comparing it with other biomarkers.
Methods: We included 122 patients with chronic liver disease or cirrhosis who underwent liver biopsy. ELF scores, calculated for each fibrosis stage (F0-F4) based on the New Inuyama Classification, were compared with platelet count, aspartate aminotransferase-to-platelet ratio index (APRI), fibrosis-4 index, Mac-2-binding protein glycan isomer (M2BPGi) levels, and autotaxin (ATX) levels.
Results: ELF scores exhibited the highest correlation with fibrosis stages determined by liver biopsy ($\rho=0.741$, $P<0.001$) compared to other biomarkers. ELF scores increased with the development of fibrosis, and were higher in F1 than in F0 ($P=0.0062$) and in F2 than in F1 ($P=0.0223$). The area under the curve (AUC) values for the ELF scores were 0.913, 0.890, 0.870, and 0.850 for ≥ F1, ≥ F2, ≥ F3, and ≥ F4, respectively. The AUC values of ELF scores were comparable to those of M2BPGi levels across all stages, surpassing ATX levels for ≥ F1, and outperforming other markers for both ≥ F1 and F2 stages. ELF scores exhibited high specificity (94.44%) for ≥ F1. For ≥ F2, sensitivity was 83.82%, specificity 81.48%. Both ≥ F3 and ≥ F4 demonstrated high sensitivity (86.96% and 90.00%, respectively).
Conclusions: The ELF score, which strongly correlated with liver fibrosis, is particularly useful for diagnosing mild and moderate chronic hepatitis in Japanese patients and has the potential to rule out advanced liver fibrosis.
〔Lab Med Int 2025; 4(1): 8-20〕

Key Words
liver fibrosis, enhanced liver fibrosis score (ELF), Mac-2 binding protein glycosylation isomer (M2BPGi), autotaxin (ATX), noninvasive biomarkers

I. Introduction

Hepatic fibrosis progression is strongly associated with the prognosis of chronic liver disease and increases the risk of esophageal varices and carcinogenesis [1) 2)]. Histological evaluation by liver biopsy has been the gold standard for assessing liver fibrosis; however, it is an invasive procedure [3) 4)] and there are reports of significantly

different inter-observer assessments [5) 6)]. It is difficult to repeat liver biopsies to observe changes in hepatic fibrosis. Therefore, noninvasive evaluation methods such as serum biomarker analysis and diagnostic imaging are used to detect the fibrosis stage [7)–9)]. The enhanced liver fibrosis score (ELF score) was originally determined by Rosenberg et al. [10)], based on age, tissue inhibitor of metalloproteinases 1 (TIMP-1), amino-terminal propeptide of type III procollagen (PIIIP), and serum hyaluronic acid (HA); it was shown to correlate with the progression of liver fibrosis as determined by liver biopsy [10)]. The utility of the ELF score based on three fibrosis markers excluding age has been previously reported and is commonly used in clinical practice [11)].

However, to date, the ELF scores have been primarily evaluated in European and American populations. In February 2024, the ELF score was incorporated into the insurance coverage framework in Japan. However, awareness among the population is limited. This study aimed to validate the efficacy of the ELF score as a noninvasive marker for assessing liver fibrosis in the Japanese population by incorporating a comprehensive comparison with alternative markers. The utility of the ELF score for assessing liver fibrosis in Japanese individuals was confirmed by Seko et al.'s 2022 report on metabolic dysfunction associated steatotic liver disease (MASLD) patients [12)]. They compared the AUC values of the ELF score, Mac-2-binding protein glycan isomer (M2BPGi) [13)], and fibrosis-4 index (Fib-4) [8)] in Japanese MASLD patients, concluding that the ELF score is superior in diagnostic accuracy, comparable to other indices. We believe that further evaluation of the ELF score's utility in Japanese individuals is necessary, and we attempted validation including liver fibrosis from more diverse etiologies. In addition to M2BPGi and Fib-4, we compared the ELF score with many more noninvasive fibrosis biomarkers. Here, we measured the ELF score in Japanese patients with chronic liver disease and cirrhosis who underwent liver biopsy and evaluated its usefulness in the diagnosis of liver fibrosis. To achieve this, we compared the ELF score with other noninvasive fibrosis biomarkers: platelet (PLT) count [14)], aspartate aminotransferase to platelet ratio index (APRI) [7)], Fib-4 index, M2BPGi, and autotaxin (ATX) [15)].

II. Subjects and methods

Patients

Between April 2015 and March 2016, 122 patients with chronic liver disease and cirrhosis underwent liver biopsy and blood sampling at the Kagawa University Hospital (53 male, 69 female; the median age with interquartile ranges [IQRs], 65.0 [54.0-74.3] years) were studied. We retrospectively examined patient case records. Based on the New Inuyama Classification [16)], we determined the number of cases at various stages of liver fibrosis (F0, no fibrosis; F1, portal fibrous widening; F2, portal fibrous widening with bridging fibrosis; F3, bridging fibrosis plus lobular distortion; and F4, liver cirrhosis) as F0=18 cases; F1=36 cases; F2=22 cases; F3=16 cases, and F4=30 cases. Liver damage results from chronic hepatitis B (CHB), chronic hepatitis C (CHC), alcohol-associated liver disease, MASLD, autoimmune hepatitis (AIH), primary biliary cholangitis (PBC), PBC-AIH overlap syndrome, and unknown causes (unknown) (**Table 1**). This retrospective study was conducted in accordance with the principles of the Declaration of Helsinki and was approved by the Ethics Committee of the Faculty of Medicine of Kagawa University (approval Number: 2016-016). Informed consent was obtained from all individuals included in this study.

Examination methods

Blood samples were collected, and PLT count and aspartate aminotransferase (AST) and alanine aminotransferase (ALT) levels were measured on the day of blood collection. The serum samples were stored at −70°C and subsequently used to measure HA, PIIIP, TIMP-1, M2BPGi levels, and ATX levels. The HA, PIIIP, and TIMP-1 serum concentrations (C_{HA}, C_{PIIIP}, and $C_{TIMP\text{-}1}$ [ng/mL]) were measured with the ADVIA Centaur XP Immunoassay System (Siemens Healthcare Diagnostics K.K., Tokyo, Japan), which is based on the principle of chemiluminescent immunoassay (CLIA). For these assays, the measurement reagents were ADVIA Centaur®Hyaluronic Acid (HA), ADVIA Centaur®N-terminal Propeptide of TypeIII Procollagen (PIIINP), and ADVIA Centaur® Tissue Inhibitor of Metalloproteinase 1 (TIMP-1) (Siemens Healthcare Diagnostics K.K., Tokyo, Japan). The M2BPGi assay was performed using the automatic immunoassay system HISCL-800 (Sysmex Corporation Kobe, Japan) and a dedicated reagent HISCL M2BPGi assay kit (Sysmex Corporation, Kobe, Japan) based on the principles of chemiluminescent enzyme immunoassay (CLEIA). The M2BPGi value was expressed in terms of the cutoff index (COI). The ATX assay was performed using a specific two-site enzyme immunoassay with the AIA-2000 system (Tosoh, Tokyo, Japan) and a dedicated reagent E test「TOSOH」II (autotaxin) (Tosoh, Tokyo, Japan).

ELF score was calculated by the formula:

"ELF score = 2.278 + 0.851In × (C_{HA}) + 0.751In ×

Table 1 Patient's characteristics.

Characteristics		Patients (N = 122)	
Sex:		53 male / 69 female patients	
Median age (IQR), years		65.0 (54.0-74.3)	
Histological Fibrosis stage	(N)	65 > median age (IQR), years (N)	65 ≦ median age (IQR), years (N)
F0	18	47.0 (31.5-54.9) (14)	75.5 (66.8-79.0) (4)
F1	36	55.0 (40.5-60.0) (20)	73.0 (69.8-79.8) (16)
F2	22	58.0 (54.0-62.3) (10)	75.5 (67.0-78.8) (12)
F3	16	54.5 (35.0-65.8) (8)	69.0 (58.3-71.8) (8)
F4	30	60.0 (50.8-71.0) (6)	76.0 (64.0-80.5) (24)
Underlying disease		N (Fibrosis stage, N)	
Chronic hepatitis B		8 (F0=4, F1=3, F2=1, F3=0, F4=0)	
Chronic hepatitis C		33 (F0=0, F1=6, F2=5, F3=6, F4=16)	
Alcohol-associated liver disease		9 (F0=1, F1=0, F2=1, F3=2, F4=5)	
Metabolic dysfunction associated steatotic liver disease		35 (F0=9, F1=10, F2=5, F3=6, F4=5)	
Autoimmune hepatitis		7 (F0=1, F1=4, F2=2, F3=0, F4=0)	
Primary biliary cholangitis		13 (F0=0, F1=5, F2=5, F3=1, F4=2)	
Primary biliary cholangitis-autoimmune hepatitis overlap syndrome		5 (F0=0, F1=2, F2=2, F3=1, F4=0)	
Unknoun		12 (F0=3, F1=6, F2=1, F3=0, F4=2)	

N: number of patients; SD: standard deviation; IQR: interquartile range

(C_{PIIIP}) + 0.394 × In ($C_{TIMP\text{-}1}$)."

The APRI was calculated using the formula:

"100 × (AST level/the upper limit of the normal value of AST [IU/L] / PLT [$\times 10^9$/L]"[7]. The upper limit of normal AST level at our hospital was 35 IU/L.

The Fib-4 index was calculated by the formula:

"Age [years] × AST [IU/L] / PLT [$\times 10^9$/L] × (ALT [IU/L]$^{1/2}$)"[8].

A pathologist made the histological diagnosis of liver biopsies based on the New Inuyama Classification[16].

ATX levels and ELF scores were evaluated both overall and separately for males and females because ATX levels reportedly sex differences[15].

Quality control

The quality controls for HA, PIIIP, and TIMP-1 were assessed using three controls with varying concentrations. The mean ± standard deviation (SD) and coefficient of variation (CV) for the three controls of HA were 18.79 ± 0.78 ng/mL (CV 4.16%), 50.81 ± 1.40 ng/mL (CV 2.75%), and 205.82 ± 6.49 ng/mL (CV 3.16%), respectively. For PIIIP, the values were 2.05 ± 0.05 ng/mL (CV 2.46%), 5.37 ± 0.15 ng/mL (CV 2.81%), and 11.97 ± 0.30 ng/mL (CV 2.52%), respectively. Similarly, for TIMP-1, the results were 90.74 ± 2.71 ng/mL (CV 2.99%), 250.84 ± 5.17 ng/mL (CV 2.06%), and 521.17 ± 13.71 ng/mL (CV 2.63%), respectively.

Statistical analysis

Data were expressed as medians with interquartile ranges (IQRs). Nonparametric Steel–Dwass analysis was used for multiple comparisons between each group of liver fibrosis stages, and for underlying illness. Receiver operating characteristic (ROC) curves were used to evaluate the performance of the ELF score and other markers in the diagnosis of liver fibrosis. In addition, the area under the curve (AUC) with 95% confidence intervals (CI), sensitivity, specificity, positive predictive value (PPV), negative predictive value (NPV), positive likelihood ratio (LR^+), and negative likelihood ratio (LR^-) were calculated from the ROC. Comparisons of the AUC were performed using the chi-square test. The optimal cutoff value was defined as the point maximizing the Youden index (=max [sensitivity+specificity-1]). The Spearman's rank correlation coefficient (ρ) was used for evaluating the correlation between liver fibrosis stages obtained from the biopsy and the individual fibrosis biomarkers (ELF score, PLT count, APRI, Fib-4 index, M2BPGi level, and ATX level). The impact of age on the ELF score was assessed by categorizing patients into two groups: those under 65 years of age and those 65 years and older at each stage of liver fibrosis. The ELF score values for these groups were then analysed for statistical significance using the Mann-Whitney U test. All statistical analyses were performed using JMP Pro 16 software (SAS Institute Inc., Cary, NC, USA). Statistical significance was defined as $P < 0.05$.

III. Results

Correlation between fibrosis stage determined by liver biopsy and six liver fibrosis markers: ELF score, PLT, APRI, Fib-4 Index, M2BPGi, and ATX

Table 2 shows the Spearman's rank correlation coefficient between the fibrosis stages determined by liver biopsy and biomarkers. Each marker significantly correlated with the fibrosis stage. PLT counts declined with increasing stage, whereas all other counts increased. The correlation with fibrosis stage showed a strong correlation ($\rho \geq 0.6$), including ATX levels by sex, except for PLT and APRI. ELF scores exhibited the highest correlation overall ($\rho=0.741$, $P<0.001$) among other biomarkers.

Comparison of biomarkers according to liver fibrosis stage

A comparison of ELF scores according to liver fibrosis stages based on the New Inuyama Classification showed that the median (IQR) ELF scores were 8.84 (8.46–9.65), 9.89 (9.25–10.75), 10.92 (10.04–11.82), 11.55 (11.01–12.01), and 12.08 (11.36–12.64) for fibrosis stages F0, F1, F2, F3, and F4, respectively. The median ELF score increased with fibrosis development. The ELF scores were higher in the F1 stage than in the F0 stage (P=0.0062). These values were also higher in the F2 stage than in the F1 stage (P=0.0223). However, there was no significant difference between the F2 and F3 stages (P=0.5090) or between the F3 and F4 stages (P=0.3282) (**Figure 1a**).

Furthermore, the median PLT counts for fibrosis stages F0, F1, F2, F3, and F4 were 21.85 10^4/μL (18.20 10^4–24.80 10^4/μL), 20.70 10^4/μL (18.25 10^4–23.90 10^4/μL), 18.00 10^4/μL (15.25 10^4–23.40 10^4/μL), and 10.70 10^4/μL (7.48 10^4–14.68 10^4/μL), respectively (**Figure 1b**). The median PLT count decreased with the development of fibrosis. PLT counts were lower in F4 stage than in F3 stage (P=0.0265), whereas PLT counts were not significantly different between any other successive fibrosis stages. The median APRI values for fibrosis stages F0, F1, F2, F3, and F4 were 0.44 (0.31–0.87), 0.68 (0.46–1.13), 0.77 (0.49–1.71), 1.75 (1.02–2.18), and 1.16 (0.56–1.75), respectively (**Figure 1c**). The median APRI did not show a constant increase in one part of the fibrosis stage and did not show significant differences between any successive fibrosis stages. The median Fib-4 indices for the fibrosis stages F0, F1, F2, F3, and F4 were 1.37 (0.73–2.21), 2.19 (1.54–3.35), 2.80 (1.37–4.73), 3.98 (2.76–5.14), and 5.07 (3.53–8.42), respectively (**Figure 1d**). The median Fib-4 index increased with the development of fibrosis. The Fib-4 index did not show significant differences between successive fibrosis stages. The median M2BPGi levels for fibrosis stages F0, F1, F2, F3, and F4 were 0.66 COI (0.47–0.89 COI), 1.32 COI (0.69–2.08 COI), 1.76 COI (1.00–4.02 COI), 3.58 COI (1.51–4.23 COI), and 4.35 COI (2.43–7.47 COI), respectively (**Figure 1e**). The median M2BPGi levels increased with the development of fibrosis. M2BPGi levels were higher in F1 stage than in F0 stage (P=0.0112), whereas M2BPGi levels were not significantly different between any of the other successive fibrosis stages. The median ATX levels in overall for fibrosis stages F0, F1, F2, F3, and F4 were 0.88 mg/L (0.68–1.06 mg/L), 0.89 mg/L (0.74–1.11 mg/L), 1.32 mg/L (0.98–1.51 mg/L), 1.54 mg/L (1.21–2.02 mg/L), 1.62 mg/L (1.21–1.85 mg/L), respectively (**Figure 1f**). The median ATX levels

Table 2 Correlation between fibrosis stage by liver biopsy and biochemical markers of hepatic fibrosis.

Biochemical markers of hepatic fibrosis		number	Correlation coefficient (ρ)	P value
ELF score	overall	122	0.741	(P<0.0001)
	Male	53	0.770	(P<0.0001)
	Female	69	0.709	(P<0.0001)
PLT	overall	116	-0.572	(P<0.0001)
APRI	overall	116	0.338	(P=0.0020)
FIB-4 Index	overall	115	0.615	(P<0.0001)
M2BPGi	overall	122	0.666	(P<0.0001)
ATX	overall	106	0.662	(P<0.0001)
	Male	45	0.771	(P<0.0001)
	Female	61	0.634	(P<0.0001)

ELF score: enhanced liver fibrosis score; PLT: platelet count; APRI: aspartate aminotransferase to platelet ratio index; M2BPGi: Mac-2 binding protein glycosylation isomer; ATX: autotaxin. The Spearman's rank correlation coefficient (ρ) was used for evaluating the correlation between liver fibrosis stages and the individual fibrosis biomarkers.

increased with the development of fibrosis. ATX levels were higher in F2 stage than in F1 stage (P=0.0133), whereas ATX levels were not significantly different between any of the other successive fibrosis stages.

ELF scores and ATX levels among liver fibrosis stages by sex

The median ELF scores in males for fibrosis stages F0, F1, F2, F3, and F4 were 8.81 (7.92–9.68), 9.54 (8.97–10.72), 11.32 (10.65–11.74), 11.55 (10.99–12.01), and 11.88 (11.26–12.41), respectively (**Figure 1g**). The median ELF scores in females with fibrosis stages F0, F1, F2, F3, and F4 were 8.86 (8.58–9.62), 10.02 (9.49–10.81), 10.79 (10.01–12.01), 11.54 (10.89–12.10), and 12.33 (11.48–12.81), respectively (**Figure 1i**). The median ELF scores in males and females increased with the development of fibrosis. The median ATX levels in males for fibrosis stages F0, F1, F2, F3, and F4 were 0.72 mg/L (0.66–0.92 mg/L), 0.72 mg/L (0.59–0.77 mg/L), 0.87 mg/L (0.83–1.32 mg/L), 1.22 mg/L (1.14–1.49 mg/L), 1.62 mg/L (1.15–1.81 mg/L), respectively (**Figure 1h**). The median ATX levels in females for fibrosis stages F0, F1, F2, F3, and F4 were 0.94 mg/L (0.82–1.16 mg/L), 1.02 mg/L (0.89–1.22 mg/L), 1.36 mg/L (1.11–1.61 mg/L), 1.90 mg/L (1.43–2.11 mg/L), and 1.62 mg/L (1.34–1.87 mg/L), respectively (**Figure 1j**). The median ATX levels in both sexes did not show a constant increase at a single stage of fibrosis. When comparing the ELF scores and ATX levels for fibrosis stages in males and females, only the ELF scores in males between F0 and F1 showed a significant difference (P=0.0229).

Ability of ELF score to predict liver fibrosis

ROC analyses aimed to assess the diagnostic accuracy of the ELF scores for the fibrosis stages. **Figure 2** illustrates the ROC curves of the ELF scores, while **Table 3a** displays the calculated values for the AUC, cutoff value, sensitivity, specificity, PPV, NPV, LR+, and LR − for each fibrosis stage. The AUC values were 0.913, 0.890, 0.870, and 0.850 for ≥ F1, ≥ F2, ≥ F3, and ≥ F4, respectively.

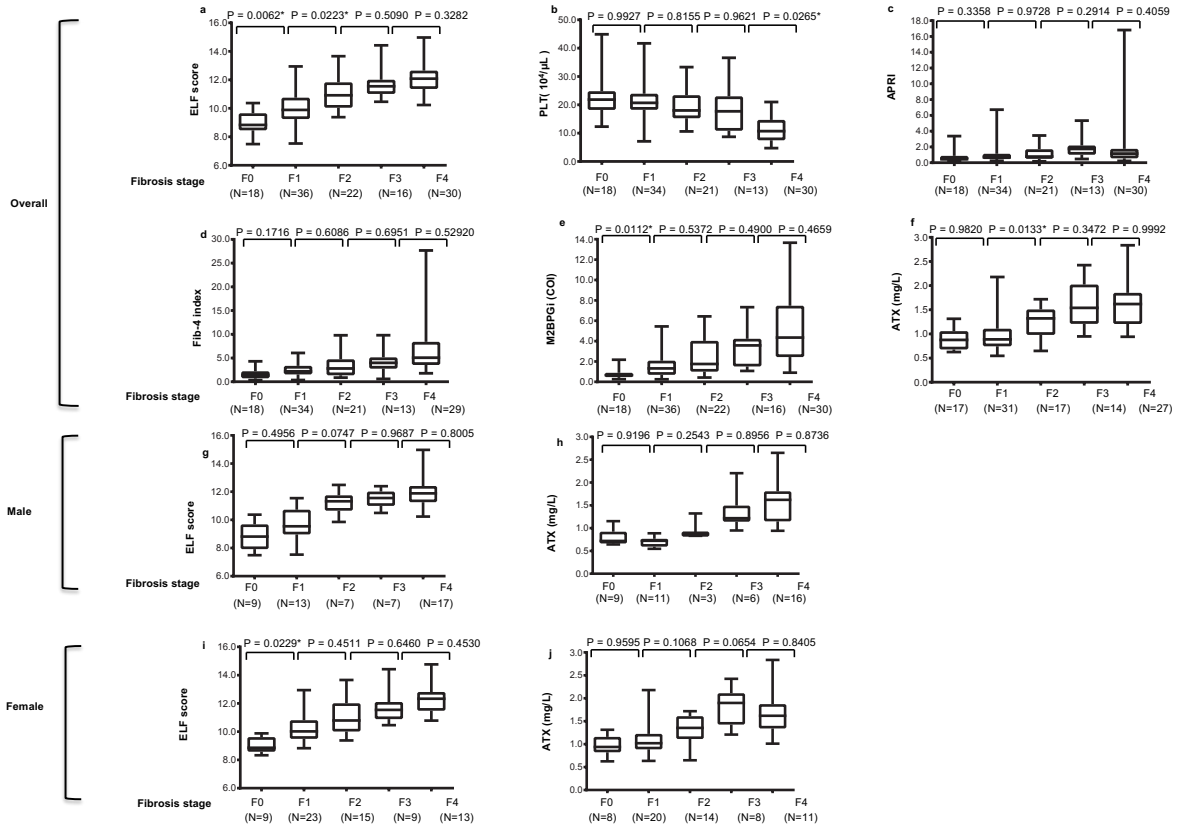

Figure 1 Comparison of biomarkers according to liver fibrosis stage.
Overall: (a) ELF score, (b) PLT, (c) APRI, (d) Fib4-index, (e) M2BPGi, and (f) ATX.
Male: (g) ELF score, (h) ATX. Female: (i) ELF score, (j) ATX.
(g) to (j) are ELF scores and ATX levels comparisons by sex.
ELF score: enhanced liver fibrosis score; PLT: platelet count; APRI: aspartate aminotransferase to platelet ratio index; M2BPGi: Mac-2 binding protein glycosylation isomer; ATX: autotaxin;
P-value*: <0.05.

The corresponding cutoff values for predicting fibrosis stages were 9.92, 10.64, 10.99, and 11.00, respectively. Notably, the cut-off values for fibrosis stages ≥ F3 and ≥ F4 were nearly identical. ELF scores exhibited high specificity (94.44%), PPV (98.80%), and LR+ (14.18) for ≥ F1. For ≥ F2, sensitivity was 83.82%, specificity 81.48%, PPV 85.07%, NPV 80.00%, LR+ 4.53, and LR- 0.20. Both ≥ F3 and ≥ F4 demonstrated high sensitivity (86.96% and 90.00%, respectively), high NPV (90.91% and 95.52%, respectively), and low LR− (0.17 and 0.14, respectively).

Comparison of fibrosis markers by AUC

Table 3a presents the AUC of the ELF score, PLT count, APRI, Fib-4 index, M2BPGi, and ATX for liver fibrosis stages, along with their corresponding values. The AUC of ELF scores for ≥ F1 was significantly higher than PLT counts (AUC=0.703, P=0.0005), APRI (AUC=0.726, P=0.0076), Fib-4 index (AUC=0.809, P=0.0354), and ATX levels (AUC=0.785, P=0.0031) and comparable to M2BPFi levels (AUC=0.880, P=0.2184). Similar to the ELF scores, the Fib-4 index, M2BPGi levels, and ATX levels displayed high specificity, PPV, and LR+ for ≥ F1. For ≥ F2, the AUC of ELF scores was significantly higher than that of PLT counts (AUC=0.763, P=0.0109), APRI (AUC=0.679, P <0.0001), and Fib-4 index (AUC=0.803, P=0.0228), and comparable to M2BPFi levels (AUC=0.830, P=0.0600) and ATX levels (AUC=0.881, P=0.7734). ELF scores exhibited the highest sensitivity, the highest NPV, and the lowest LR- among the markers for ≥ F2, while the specificity of APRI (84.62%), M2BP-Gi levels (88.89%), and ATX levels (87.50%) surpassed that of ELF scores. For fibrosis stages ≥ F3 and ≥ F4, the AUC of ELF scores was significantly higher than APRI but comparable to other biomarkers. ELF scores had the highest sensitivity, the highest NPV, and the lowest LR- among the markers for ≥ F3, while specificity was similar to Fib4-index (79.45%) and M2BPGi levels (81.58%). For ≥ F4, PLT counts (93.33%) and the Fib4-index (89.66%) showed comparable sensitivity to ELF scores. However, the cutoff values for PLT, APRI, Fib-4, M2BPGi, and ATX either exhibited nearly consistent values across stages or showed a reversal between stages.

Diagnostic ability of ELF score and ATX for predicting liver fibrosis stages by sex

Comparisons of the AUC between ELF scores and ATX levels in predicting fibrosis stage by sex are presented in

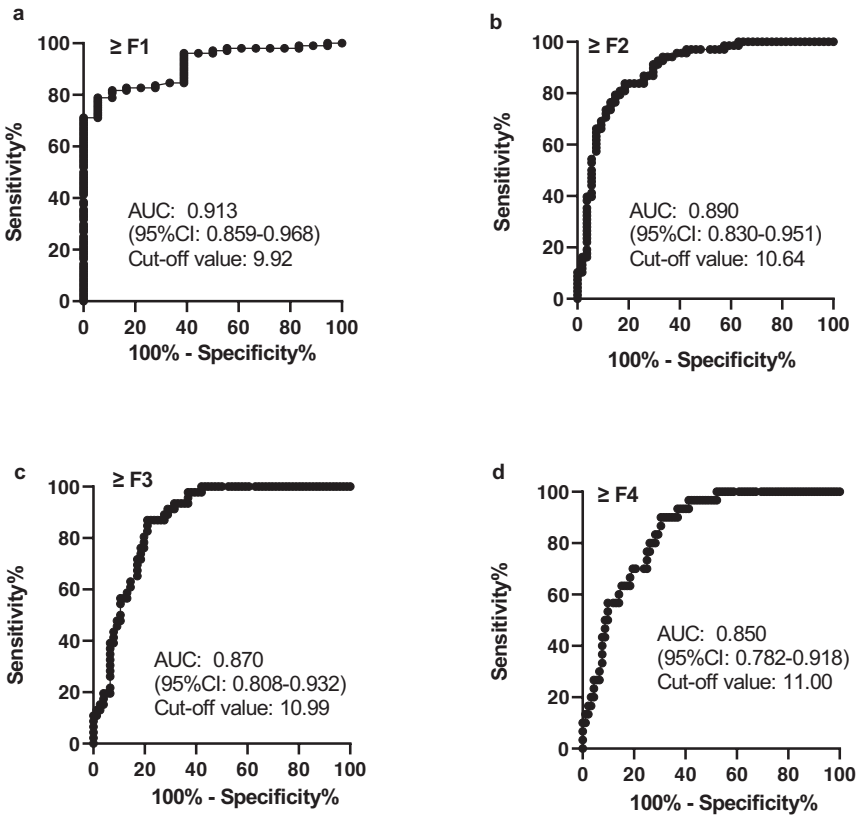

Figure 2 The ROC curves of ELF scores.

(a) For ≥ liver fibrosis stage F1, (b) for ≥ F2, (c) for ≥ F3, and (d) for ≥ F4. ROC: receiver operating characteristic; AUC: area under the curve; CI: confidence interval. The cutoff value was defined as the point maximizing the Youden index.

Table 3 a Diagnostic performance of fibrosis biochemical markers in overall.

Liver fibrosis stage	Fibrosis biochemical Marker	AUC (95% CI)	Cut-off value	Sensitivity [%]	Specificity [%]	PPV [%]	NPV [%]	P value	LR+	LR-
≥ F1	ELF score	0.913 (0.859-0.968)	9.92	78.85	94.44	98.80	43.59	–	14.18	0.22
	PLT [×10⁴/μL]	0.703 (0.592-0.813)	18.00	55.10	83.33	94.74	25.42	0.0005*	3.31	0.54
	APRI	0.726 (0.598-0.855)	0.43	88.78	50.00	90.63	45.00	0.0076*	1.78	0.22
	Fib-4 index	0.809 (0.711-0.908)	3.08	55.67	94.44	98.18	14.00	0.0354*	10.01	0.47
	M2BPGi [COI]	0.880 (0.810-0.949)	1.20	74.04	94.44	98.72	38.64	0.2184	13.32	0.27
	ATX [mg/L]	0.785 (0.689-0.880)	1.16	58.43	94.12	98.11	30.19	0.0031*	9.94	0.44
≥ F2	ELF score	0.890 (0.830-0.951)	10.64	83.82	81.48	85.07	80.00	–	4.53	0.20
	PLT [×10⁴/μL]	0.763 (0.675-0.851)	18.00	71.88	78.85	80.70	69.49	0.0109*	3.40	0.36
	APRI	0.679 (0.576-0.774)	1.19	51.56	84.62	80.49	58.67	<0.0001*	3.35	0.57
	Fib-4 index	0.803 (0.724-0.883)	2.50	80.95	71.15	77.27	75.51	0.0228*	2.81	0.27
	M2BPGi [COI]	0.830 (0.758-0.902)	2.18	64.71	88.89	88.00	66.67	0.0600*	5.82	0.40
	ATX [mg/L]	0.881 (0.816-0.946)	1.21	75.86	87.50	88.00	75.00	0.7734	6.07	0.28
≥ F3	ELF score	0.870 (0.808-0.932)	10.99	86.96	78.95	71.43	90.91	–	4.13	0.17
	PLT [×10⁴/μL]	0.824 (0.740-0.909)	17.30	79.07	75.34	65.38	85.94	0.3656	3.21	0.28
	APRI	0.691 (0.592-0.790)	1.10	62.79	73.97	58.70	77.14	0.0002*	2.41	0.50
	Fib-4 index	0.828 (0.750-0.906)	3.49	78.57	79.45	68.75	86.57	0.2762	3.82	0.27
	M2BPGi [COI]	0.845 (0.776-0.913)	2.19	76.09	81.58	71.43	84.93	0.4328	4.13	0.29
	ATX [mg/L]	0.865 (0.799-0.932)	1.21	82.93	75.38	68.00	87.50	0.8946	3.37	0.23
≥ F4	ELF score	0.850 (0.782-0.918)	11.00	90.00	69.57	49.09	95.52	–	2.96	0.14
	PLT [×10⁴/μL]	0.891 (0.831-0.951)	17.20	93.33	73.26	54.90	96.92	0.3268	3.49	0.09
	APRI	0.606 (0.492-0.719)	0.85	66.67	56.98	35.09	83.05	<0.0001*	1.55	0.58
	Fib-4 index	0.832 (0.754-0.911)	2.95	89.66	62.79	44.83	94.74	0.6419	2.41	0.16
	M2BPGi [COI]	0.829 (0.751-0.908)	2.19	80.00	72.83	48.98	91.78	0.5590	2.94	0.27
	ATX [mg/L]	0.798 (0.709-0.887)	1.34	74.07	78.48	54.05	89.86	0.2538	3.44	0.33

CI: confidence interval; PPV: positive predictive value; NPV: negative predictive value; LR+: positive likelihood ratio; LR-: negative likelihood ratio; ELF score: enhanced liver fibrosis score; PLT count: platelet count; APRI: aspartate aminotransferase to platelet ratio index; M2BPGi: Mac-2 binding protein glycosylation isomer; ATX: autotaxin; P value: the AUC of ELF score versus that of other fibrosis marker, and P value*: < 0.05.

Table 3b Diagnostic performance of ELF score and ATX by sex.

Liver fibrosis stage	Fibrosis biochemical Marker		AUC (95% CI)	Cut-off value	Sensitivity [%]	Specificity [%]	PPV [%]	NPV [%]	P value	LR+	LR-
≥ F1	ELF score	・Female	0.925 (0.856-0.995)	9.92	78.33	100.00	100.00	40.91	–	1.00	0.22
		Male	0.909 (0.829-0.990)	10.49	77.27	100.00	100.00	47.37	–	1.00	0.23
	ATX [mg/L]	・Female	0.778 (0.643-0.914)	1.16	64.15	87.50	97.14	26.92	0.0066*	5.13	0.41
		Male	0.772 (0.630-0.914)	1.21	50.00	100.00	100.00	33.33	0.0295*	1.00	0.50
≥ F2	ELF score	・Female	0.845 (0.750-0.940)	10.70	78.38	81.25	82.86	76.47	–	4.18	0.27
		Male	0.947 (0.892-1.000)	10.91	83.87	90.91	92.86	80.00	–	9.23	0.18
	ATX [mg/L]	・Female	0.849 (0.747-0.950)	1.34	69.70	92.86	92.00	72.22	0.9388	9.76	0.33
		Male	0.968 (0.926-1.000)	0.94	92.00	90.00	92.00	90.00	0.5044	9.20	0.09
≥ F3	ELF score	・Female	0.863 (0.770-0.947)	10.70	95.45	70.21	60.00	97.06	–	3.20	0.06
		Male	0.890 (0.803-0.977)	10.99	87.50	79.31	77.78	88.46	–	4.23	0.16
	ATX [mg/L]	・Female	0.863 (0.764-0.963)	1.55	73.68	88.10	73.68	88.10	0.9898	6.19	0.30
		Male	0.966 (0.919-1.000)	0.94	100.00	86.96	88.00	100.00	0.0227*	7.67	0.00
≥ F4	ELF score	・Female	0.864 (0.775-0.953)	10.78	100.00	62.50	38.24	100.00	–	2.67	0.00
		Male	0.851 (0.748-0.954)	11.06	88.24	69.44	57.69	92.59	–	2.89	0.17
	ATX [mg/L]	・Female	0.755 (0.606-0.903)	1.55	72.73	78.00	42.11	92.86	0.1501	3.31	0.35
		Male	0.904 (0.817-0.992)	1.01	93.75	75.86	68.18	95.65	0.3255	3.88	0.08

Table 3b. For fibrosis stages ≥ F1, the AUC of ELF scores was significantly higher than that of ATX levels in both males and females. ELF scores in both sexes and ATX levels in males were shown to have high specificity (100.00%) and PPV (100.00%) for ≥ F1, whereas the specificity of ATX levels in females was 87.50%. For fibrosis stages ≥ F2, ≥ F3, and ≥ F4, the AUC of ELF scores was comparable to that of ATX levels in both sexes. For ≥ F2 in females, the specificity (92.86%) of ATX levels was higher than that of the ELF scores (81.25%). For ≥ F2 in males, the sensitivity (92.00%) of ATX levels was higher than that of ELF scores (83.87%), and the specificity (90.00%) of ATX levels was similar to that of ELF scores (90.91%). For ≥ F3 in females, the sensitivity (94.45%) of the ELF scores was higher than that of the ATX levels (73.68%). For ≥ F3 in males, the sensitivity (100.00%) of ATX levels was higher than that of ELF scores (87.50%). Similarly, for ≥ F4 in females, the sensitivity (100.00%) of ELF scores was higher than that of ATX levels (72.23%), and for ≥ F4 in males, the sensitivity (93.75%) of ATX levels was higher than that of ELF scores (88.24%). However, the cut-off values for the ELF score and ATX in both sexes were almost indistinguishable between the stages.

Comparison of fibrosis markers and their etiologies

CHC group and MASLD group were analyzed independently, and CHB, alcohol-associated liver disease, AIH, PBC, PBC-AIH overlap syndrome, and unknown etiologies were grouped together as grouped categories. **Figure 3** presents a comparison of marker values among the CHC group, MASLD group, and grouped categories in F1-F2 and F3-F4 stages, respectively. The median (IQR) ELF scores in F1-F2 and F3-F4 stages were 11.14 (10.91-11.54) and 11.87 (11.07-12.35) for the CHC group, 9.85 (9.18-10.65) and 11.99 (11.47-13.11) for the MASLD group, and 10.03 (9.48-10.79) and 12.01 (11.09-12.30) for

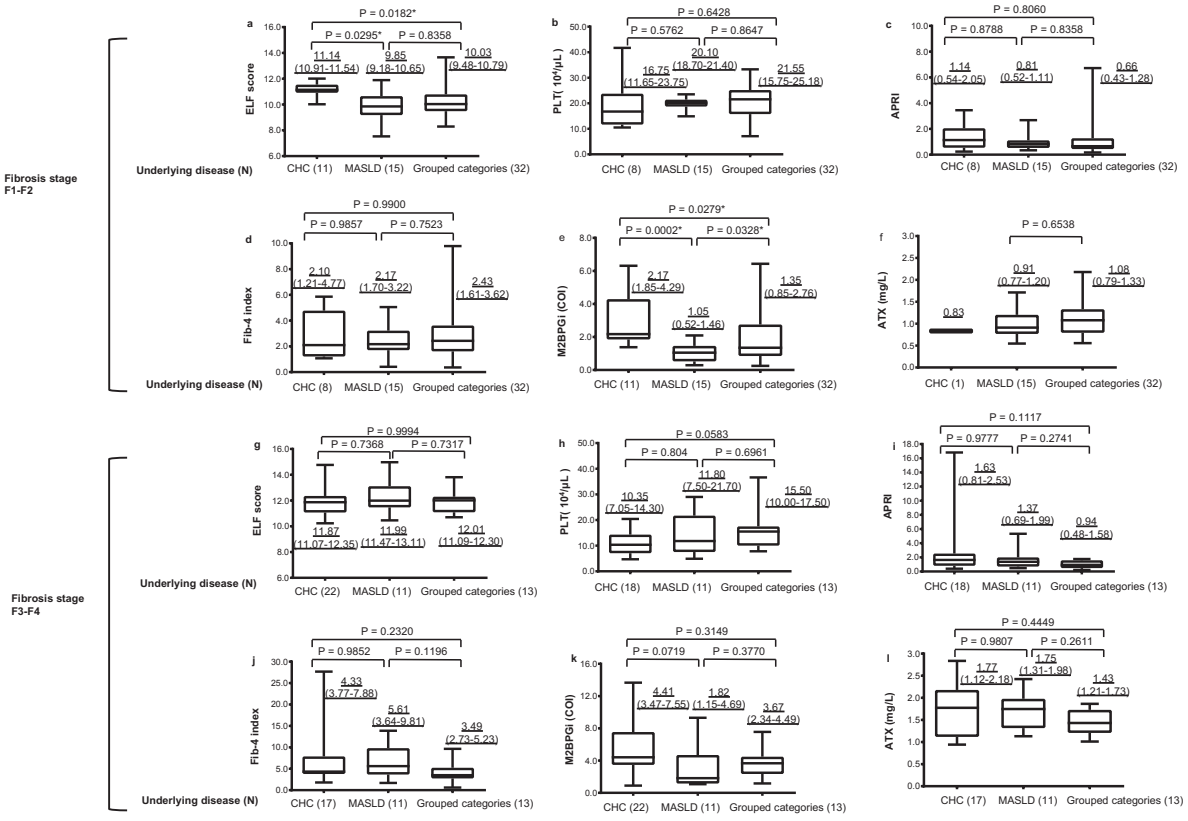

Figure 3 Comparison of fibrosis markers and their etiologies

Fibrosis stage F1 -F2: (a) ELF score, (b) PLT, (c) APRI, (d) Fib4-index, (e) M2BPGi, and (f) ATX.

Fibrosis stage F3 -F4: (g) ELF score, (h) PLT, (i) APRI, (j) Fib4-index, (k) M2BPGi, and (l) ATX.

ELF score: enhanced liver fibrosis score; PLT: platelet count; APRI: aspartate aminotransferase to platelet ratio index; M2BPGi: Mac-2 binding protein glycosylation isomer; ATX: autotaxin; CHC: chronic hepatitis C; MASLD: metabolic dysfunction associated steatotic liver disease; P-value*:<0.05.

CHB, alcohol-associated liver disease, AIH, PBC, PBC-AIH overlap syndrome, and unknown etiologies were grouped together as grouped categories. The underlined numbers in the figure indicate the median and interquartile ranges of the marker for each underlying disease.

grouped categories, respectively. Nonparametric Steel–Dwass analysis revealed that the ELF scores of the CHC group in the F1-F2 stages were significantly higher than those of the MASLD group (P = 0.0295) and the grouped categories (P = 0.0182). However, there was no significant difference between the MASLD group and the grouped categories (P = 0.8358). In the F3-F4 stages, the ELF scores did not show significant differences among any of the groups. Similarly, the M2BPGi levels in the CHC group during the F1-F2 stages were significantly elevated compared to the MASLD group (P = 0.0002) and the grouped categories (P = 0.0279). The grouped categories also exhibited significantly higher M2BPGi levels than the MASLD group (P = 0.0328). In contrast, no significant differences in M2BPGi levels were observed among any of the groups in the F3-F4 stages. For other markers, no significant differences were observed among the three etiological groups at either the F1-F2 or F3-F4 stages. **Table 4** presents the AUC, cut-off values, sensitivity, specificity, PPV, and NPV of the ELF scores and M2BPGi across different stages of liver fibrosis within each of the three etiological groups. The AUC of the ELF scores were fair for CHC with fibrosis stages ≥ F3 (AUC = 0.729) and ≥ F4 (AUC = 0.739), but were otherwise good or excellent for all etiological groups, with AUC ranging from 0.809 to 0.936. The AUC of M2BPGi were fair for MASLD with fibrosis stage ≥ F1 (AUC = 0.784), grouped categories with fibrosis stage ≥ F2 (AUC = 0.749), and CHC with fibrosis stage ≥ F3 (AUC = 0.773), but poor for CHC with fibrosis stage ≥ F4 (AUC = 0.684). The AUC for all other etiological groups were good or excellent, ranging from 0.820 to 0.947. The cutoff value of the ELF scores, calculated using AUC, was higher in the CHC group compared to other groups for fibrosis stages ≥ F2 to ≥ F4. Specifically, the cutoff values for CHC, MASLD, and grouped categories were 11.57, 10.65, and 10.01, respectively, for stage ≥ F2. The CHC group also had a higher cutoff value in M2BPGi compared to other groups. In the MASLD group, the ELF scores demonstrated high specificity for stage ≥ F1 (88.89% for MASLD and 100% for grouped categories). For stage ≥ F2,

Table 4 Diagnostic performance of ELF score and M2BPGi within each of the three etiological groups

Liver fibrosis stage	Underlying disease	Fibrosis biochemical Marker	AUC (95% CI)	Cut-off value	Sensitivity [%]	Specificity [%]	PPV [%]	NPV [%]
≥ F1	MASLD	ELF score	0.863 (0.743-0.984)	9.69	76.92	88.89	95.24	57.14
		M2BPGi [COI]	0.784 (0.636-0.933)	1.20	57.69	100	100.00	45.00
	Grouped categories	ELF score	0.899 (0.801-0.996)	9.92	68.89	100	100.00	39.13
		M2BPGi [COI]	0.863 (0.742-0.984)	0.98	80.00	88.89	97.30	47.06
≥ F2	CHC	ELF score	0.809 (0.656-0.962)	11.57	59.26	100.00	100.00	35.29
		M2BPGi [COI]	0.895 (0.786-1.000)	3.36	77.78	100.00	100.00	50.00
	MASLD	ELF score	0.934 (0.854-1000)	10.65	81.25	94.74	92.86	85.71
		M2BPGi [COI]	0.883 (0.767-0.999)	1.07	93.75	73.68	75.00	93.33
	Grouped categories	ELF score	0.870 (0.770-0.971)	10.01	92.00	72.41	76.67	91.67
		M2BPGi [COI]	0.749 (0.616-0.882)	2.18	60.00	82.76	75.00	70.59
≥ F3	CHC	ELF score	0.729 (0.559-0899)	11.80	59.09	90.91	92.86	52.63
		M2BPGi [COI]	0.773 (0.601-0.944)	3.36	81.82	72.73	85.71	66.67
	MASLD	ELF score	0.936 (0.859-1.000	11.30	90.91	87.5	76.92	95.45
		M2BPGi [COI]	0.875 (0.759-0.992)	1.07	100.00	62.5	55.00	100.00
	Grouped categories	ELF score	0.869 (0.773-0.965)	10.70	100.00	78.05	59.09	100.00
		M2BPGi [COI]	0.837 (0.728-0.946)	3.45	69.23	87.8	64.29	90.00
≥ F4	CHC	ELF score	0.739 (0.562-0.916)	11.87	62.50	82.35	76.92	70.00
		M2BPGi [COI]	0.684 (0.497-0.871)	7.44	37.50	100	100.00	62.96
	MASLD	ELF score	0.900 (0.783-1.000)	11.30	100.00	73.33	38.46	100.00
		M2BPGi [COI]	0.947 (0.872-1.000)	1.70	100.00	86.67	55.56	100.00
	Grouped categories	ELF score	0.874 (0.782-0.966)	10.78	100.00	75.56	45.00	100.00
		M2BPGi [COI]	0.820 (0.686-0.953)	3.67	66.67	86.67	50.00	92.86

AUC: area under the curve; CI: confidence interval; PPV: positive predictive value; NPV: negative predictive value; ELF score: enhanced liver fibrosis score; M2BPGi: Mac-2 binding protein glycosylation isomer; CHC: chronic hepatitis C; MASLD: metabolic dysfunction associated steatotic liver disease. CHB, alcohol-associated liver disease, AIH, PBC, PBC-AIH overlap syndrome, and unknown etiologies were grouped together as grouped categories. The cutoff value was defined as the point maximizing the Youden index.

the sensitivity and specificity in MASLD were 81.25% and 94.74%, respectively, and for stage ≥ F3, the sensitivity was 90.91% and specificity was 87.50%. In grouped categories, the sensitivity and specificity for stage ≥ F2 were 92.00% and 72.41%, respectively, and for stage ≥ F3, 100.00% and 78.05%. For stage ≥ F4, both MASLD and the grouped categories demonstrated high sensitivity (100.00%). In contrast, the ELF scores for the CHC group exhibited lower sensitivities (59.09% to 62.50%) and higher specificities (82.35% to 100.0%) for stages ≥ F2 to ≥ F4. Due to the large difference between the overall and CHC group cutoff values in the ELF scores at ≥ F2, the sensitivity and specificity for CHC were calculated using the overall cutoff value (10.64), resulting in 92.59% and 16.67%, respectively. Additionally, because the difference between the overall and grouped categories cutoff values in the ELF scores at ≥ F2 was larger than at other fibrosis stages, the sensitivity and specificity for each disease were compared using both the overall and grouped categories cutoff values. For ≥ F2, the sensitivity/specificity for PBC and PBC-AIH overlap syndrome were 63.63%/100.00% using the overall cutoff (10.64) and 81.82%/100.00% using the grouped categories cutoff (10.01). Similarly, the sensitivity/specificity for AIH and PBC-AIH overlap syndrome, Unknown etiologies, CHB, and alcohol-associated liver disease were 80.00%/100.00% and 100.00%/71.43%, 100.00%/77.78% and 100.00%/55.56%, 100.00%/85.71% and 100.00%/85.71%, and 100.00%/100.00% and 100.00%/100.00%, respectively.

The impact of age on the ELF scores

The median (IQR) ELF scores for individuals under 65 years were 8.60 (7.93-9.66), 9.52 (9.02-10.74), 10.50 (9.76-11.66), 11.32 (11.01-10.91), and 12.34 (11.70-12.57) for fibrosis stages F0, F1, F2, F3, and F4, respectively. For those aged 65 years and older, the median (IQR) ELF scores were 9.62 (9.15-10.19), 10.29 (9.59-10.87), 11.45 (10.42-11.99), 11.77 (11.85-12.16), and 11.97 (11.32-12.69) for the corresponding fibrosis stages. There was no significant difference in the median ELF scores between the under 65 and 65 and older groups at any stage of liver fibrosis (P=0.1419 for F0, P=0.0887 for F1, P=0.1593 for F2, P=0.5054 for F3, P=0.6674 for F4).

IV. Discussion

In the present study of a sample of Japanese patients with liver disease, we evaluated ELF scores for the diagnosis of the stage of liver fibrosis and compared ELF scores with other noninvasive fibrosis markers such as PLT counts [14], APRI [7], Fib-4 index [8], M2BPGi levels [13], and ATX levels [15]. ELF scores had the highest correlation coefficient with liver fibrosis among other biomarkers (ρ=0.741, P<0.001). The ELF score could distinguish the fibrosis stages more clearly than the other biomarkers. ELF scores showed high AUC (≥ 0.8) at all stages, and good diagnostic ability was obtained. Using the AUC method, the ELF score could be used to detect mild (F1) liver fibrosis with high specificity (94.44%) and to exclude severe/cirrhotic (F3-F4) liver fibrosis with high sensitivity (86.96%). This suggests that the ELF score is an alternative marker for distinguishing mild or severe liver fibrosis and is a better marker than other noninvasive markers.

Overall, ELF scores showed the highest correlation with the fibrosis stage among other biomarkers. A previous study also reported a strong correlation between ELF scores and histological fibrosis in PBC patient was strong [17]. These facts suggest that ELF scores most accurately reflect liver fibrosis among other noninvasive biomarkers.

The overall median ELF scores, Fib-4 index, M2BPGi levels, and total ATX levels tended to increase, while PLT counts decreased with the progression of liver fibrosis. Among the successive fibrosis stages, the ELF scores were significantly different only between the F0 and F1 stages and between the F1 and F2 stages. The ability of ELF scores to distinguish the early stages of fibrosis suggests their clinical utility in identifying patients at different risk levels. There was no significant difference between the F2 and F3 stages or between the F3 and F4 stages. However, a previous study in Japanese patients reported that ELF scores increased with the development of liver fibrosis and showed significant differences among all fibrosis stages (P <0.05) [18]. This discrepancy may be attributed to the small sample size used in this study. However, among other markers, only PLT counts (F3-F4), M2BPGi level (F0-F1), and total ATX level (F1-F2) could significantly differentiate between the fibrosis stages. These results suggest that the ELF score can more clearly distinguish the early stages of fibrosis than other markers, but PLT counts can more clearly distinguish cirrhosis than other markers.

When comparing ELF scores and ATX levels for liver fibrosis stages, these were evaluated separately for males and females, as there are sex differences in ATX levels [15]. In both sexes, the median ELF scores increased with the progression of liver fibrosis; however, the median ATX levels did not consistently increase with the development of fibrosis at any stage. In the analysis of ELF scores and ATX levels across liver fibrosis stages by sex, there were no significant differences between males, except for the

ELF scores between F0 and F1. In previous studies, ATX levels were observed to increase with the progression of liver fibrosis in both males and females, with significant differences between each stage [19].

We assessed the diagnostic accuracy of ELF scores for predicting various fibrosis stages and compared them with those of other fibrosis markers using AUC. ELF scores demonstrated excellent diagnostic accuracy for identifying fibrosis stages ≥ F1, ≥ F2, and ≥ F3, with AUC values of 0.913, 0.890, and 0.870, respectively. The AUC for ≥ F4 was good at 0.850. The consistently high AUC values suggest that ELF scores are effective in distinguishing between the different fibrosis stages. ELF scores demonstrated high specificity, PPV and LR+ for ≥ F1, suggesting that ELF scores are particularly reliable in the definitive diagnosis of mild (F1) liver fibrosis. For ≥ F2, ELF scores had a balanced sensitivity and specificity. This balance is crucial for accurate identification of patients with moderate fibrosis. For ≥ F3 and ≥ F4, the ELF scores showed high sensitivity and NPV. These findings suggested their effectiveness in ruling out advanced fibrosis and cirrhosis. Previous studies have shown that the ELF score has accurate diagnostic performance in CHC, MASLD, and PBC cases in European and American populations [20-22]. In Japan, Seko et al. reported that in a study of 371 Japanese patients with MASLD, the AUC of the ELF scores for stages ≥ F1, ≥ F2, ≥ F3, and ≥ F4 were 0.825, 0.817, 0.802, and 0.812, respectively [12].

ELF scores showed significantly higher AUC values for ≥ F1 than for PLT counts, APRI, Fib-4 index, and ATX levels. Similar AUC values were observed compared to the M2BPGi levels. For ≥ F2, ELF scores had significantly higher AUC than PLT counts, APRI, and Fib-4 index, and similar AUC to M2BPGi levels and ATX levels. For ≥ F3 and ≥ F4, the ELF scores had AUC values comparable to those of the other biomarkers, except for APRI. ELF scores had the highest sensitivity among the markers for ≥ F2 and ≥ F3, emphasizing their ability to detect moderate and advanced fibrosis. These results suggest that ELF scores are strong predictors of liver fibrosis, especially in the moderate to advanced stages. The ELF scores outperformed or showed a similar performance to other fibrosis markers, indicating their reliability in clinical practice. ELF scores, with their high sensitivity and specificity, may be valuable in noninvasive fibrosis assessment and could aid in clinical decision-making, reducing reliance on invasive procedures, such as liver biopsy. In this study, the AUC of ELF scores and M2BPGi levels were comparable. However, the cut-off value of M2BPGi levels remained nearly constant from F2 to F4, rendering it impractical for clinical use. A previous study reported that the ELF score and M2BPGi level exhibited nearly equivalent performances in ROC analysis among patients with hepatitis B. However, variations in performance were observed based on the chosen cutoff value [23].

The AUC of the ELF scores for predicting ≥ F1 was significantly higher than that of the ATX levels in both males and females. This suggests that the ELF scores are more effective in distinguishing the early stages of fibrosis in both sexes. The AUC of ELF scores for ≥ F2, ≥ F3, and ≥ F4 were comparable to that of ATX levels in both males and females. This implies that ELF scores and ATX levels have similar diagnostic accuracies in identifying moderate fibrosis, advanced fibrosis, and cirrhosis. ELF scores generally outperform ATX levels in predicting early fibrosis stages (≥ F1) in both sexes, while their performance becomes comparable in advanced stages. In this study, the cutoff values for ELF scores and ATX levels in both sexes were nearly identical for every fibrosis stage and were deemed impractical for clinical use. In previous studies, the cutoff values for ATX levels in both sexes showed clear differences between each stage, increasing with the progression of liver fibrosis stages [19].

In this study, a range of underlying diseases was included, necessitating an examination of their influence on the observed parameters. Notably, the impact of these diseases was evident in the ELF scores and M2BPGi levels during the early stages of fibrosis (F1-F2). Specifically, the CHC group demonstrated significantly higher values compared to other disease groups. ELF scores and M2BPGi values may vary depending on the specific underlying disease.

When evaluating the AUC by segregating the CHC group, MASLD group, and other grouped categories, the ELF scores were favorable across all disease categories. Seko et al. reported that the AUC was 0.8 or higher across all stages of liver fibrosis in patients with MASLD, which aligns with our findings. Additionally, they identified the cut-off values of the ELF test for fibrosis stages ≥ F1, ≥ F2, ≥ F3, and ≥ F4 as 9.10, 10.11, 11.10, and 11.54, respectively, which are consistent with our results of 9.69, 10.65, 11.30, and 11.30 [12]. For both the ELF scores and M2BPGi levels, the cutoff values determined by AUC for the CHC group were higher at each fibrosis stage compared to the overall cohort and other disease groups. Using an overall ELF score cutoff value of ≥ F2 for the CHC group results in low specificity, leading to a high number of false positives. Therefore, it is challenging to apply the overall cutoff value of the ELF score to the CHC group.

The MASLD group and other grouped categories demonstrated high specificity for fibrosis stages ≥ F1, with overall trends showing similar specificity. For stages ≥ F2, both sensitivity and specificity were comparable across the groups, aligning with the overall trends. Additionally, they tended to exhibit high sensitivity for stages ≥ F3 and ≥ F4. However, this pattern was not observed in the CHC group. When comparing the sensitivity and specificity of each disease within the grouped categories for fibrosis stage ≥ F2 using both the overall cutoff values and the cutoff values obtained for the grouped categories, the following observations were made: In the PBC group, the cutoff values obtained for the grouped categories demonstrated higher sensitivity. However, in the AIH group and the unknown group, the grouped categories exhibited lower specificity. No other major differences were noted.

To evaluate the impact of age on ELF scores, we analyzed the ELF scores of patients under 65 years and those over 65 years at each fibrosis stage. No significant differences were found at any stage, indicating that age does not have a significant influence on ELF scores.

This study had several limitations. The small sample sizes may have contributed to the lack of significant differences between successive fibrosis stages and the indistinguishable cutoff values for some markers across stages. Larger studies are required to validate these findings. Future studies should investigate the utility of ELF scores in diagnosing advanced liver fibrosis or cirrhosis. The participants had various etiologies of liver fibrosis, which might have influenced the ELF scores. Future studies should evaluate the usefulness of ELF scores for individual etiologies.

V. Conclusion

In conclusion, ELF scores demonstrated the highest correlation with liver fibrosis stages among noninvasive biomarkers and provided excellent diagnostic accuracy for identifying fibrosis stages. They were particularly effective in distinguishing early fibrosis stages and showed high sensitivity and specificity for advanced stages. Despite some limitations, ELF scores outperformed or showed comparable performance to other fibrosis markers, making them a reliable tool in clinical practice for noninvasive fibrosis assessment. Future studies with larger sample sizes and focused on specific etiologies are warranted to further validate these findings and expand the clinical utility of ELF scores in liver fibrosis diagnosis.

Declaration of competing interests: None declared.

Author Contributions: NK, **KF** and **TM** conceived the study concept and design. **KF** obtained approval from the Ethics Committee. **KF**, **JT**, **AM**, **KO**, **TT**, **HK**, and **TM** were involved in patient recruitment and data acquisition. **NK** was involved in data acquisition and analysis, and drafted the manuscript. **TM** supervised the study. **All authors** reviewed and revised the manuscript, and approved the final version.

Informed consent: Informed consent was obtained from all individuals included in this study. For patients who died and had no relatives listed in their clinical records, we provided opt-out methods for the relatives of the dead participants by publishing a summary of this study on our university website.

Ethical approval: This study was approved by the authors' Institutional Review Board (The Ethics Committee, Faculty of Medicine, Kagawa University) dated June 1st, 2016 (approval number: 2016-016). It complied with all relevant national regulations and institutional policies, and was in accordance with the tenets of the Helsinki Declaration (as revised in 2013).

Disclosure of Conflicts of Interest: The authors declare no conflicts of interest associated with this manuscript.

Funding: This work was financially supported by the Sysmex Corporation (Kobe, Japan) and Siemens Healthcare Diagnostics K.K. (Tokyo, Japan).

Acknowledgements: We thank Editage (www.editage.com) for English language editing.

References

1) Tada T, Kumada T, Toyoda H, et al. Long-term prognosis of patients with chronic hepatitis C who did not receive interferon-based therapy: causes of death and analysis based on the FIB-4 index. J Gastroenterol 2016; 51 (4): 380-9.
2) Angulo P, Kleiner DE, Dam-Larsen S, et al. Liver fibrosis, but no other histologic features, is associates with long-term outcomes of patients with nonalcoholic fatty liver disease. Gastroenterology 2015; 149 (2): 389-97.
3) Van der Poorten D, Kwok A, Lam T, et al. Twenty-year audit of percutaneous liver biopsy in a major australian teaching hospital. Intern Med J 2006; 36 (11): 692-9.
4) Cadranel JF, Rufat P, Degos F. Practices of liver biopsy in France: results of a prospective natiowide survey. For the

group of epidemiology of the french association for the study of the liver (AFEF). Hepatology 2000; 32 (3): 477–81.
5) Regev A, Berho M, Jeffers LJ, et al. Sampling error and intraobserver variation in liver biopsy in patients with chronic HCV infection. Am J Gastroenterol 2002; 97:2614–8.
6) Rousselet MC, Michalak S, Dupré F, et al. Sources of variability in histological scoring of chronic viral hepatitis. Hepatology 2005; 41 (2): 257-64.
7) Wai CT, Greenson JK, Fontana RJ, et al. A simple noninvasive index can predict both significant fibrosis and cirrhosis in patients with chronic hepatitis C. Hepatology 2003; 38 (2): 518-26.
8) Vallet-Pichard A, Mallet V, Nalpas B, et al. FIB-4: an inexpensive and accurate marker of fibrosis in HCV infection. Comparison with liver biopsy and fibrotest. Hepatology 2007; 46 (1): 32-6.
9) Yoshioka K, Hashimoto S. Can non-invasive assessment of liver fibrosis replace liver biopsy? Hepatol Res 2012; 42 (3): 233-40.
10) Rosenberg WM, Voelker M, Thiel R, et al. Serum markers detect the presence of liver fibrosis: a cohort study. Gastroenterology 2004; 127 (6): 1704-13.
11) Guha IN, Parkes J, Roderick P, et al. Noninvasive markers of fibrosis in nonalcoholic fatty liver disease: validating the european liver fibrosis panel and exploring simple markers. Hepatology 2008; 47 (2): 455-60.
12) Seko Y, Takahashi H, Toyoda H, et al. Diagnostic accuracy of enhanced liver fibrosis test for nonalcoholic steatohepatitis-related fibrosis: Multicenter study. Hepatol Res 2022; 53 (4): 312-21.
13) Kuno A, Ikehara Y, Tanaka Y, et al. A serum "sweet-doughnut" protein facilitates fibrosis evaluation and therapy assessment in patients with viral hepatitis. Sci Rep 2013; 3: 1065.
14) Afdhal N, McHutchison J, Brown R, et al. Thrombocytopenia associated with chronic liver disease. J Hepatol 2008; 48 (6): 1000-7.
15) Pleli T, Martin D, Kronenberger B, et al. Serum autotaxin is a parameter for the severity of liver cirrhosis and overall survival in patients with liver cirrhosis — a prospective cohort study. Plos One 2014; 9 (7): e103532.
16) Ichida F, Tsuji T, Omata M, et al. New Inuyama classification; new criteria for histological assessment of chronic hepatitis. International Hepatology Communications 1996; 6 (2): 112-9.
17) Mayo MJ, Parkes J, Adams-Huet B, et al. Prediction of clinical outcomes in primary biliary cirrhosis by serum enhanced liver fibrosis assay. Hepatology 2008; 48 (5): 1549-57.
18) Takashima T, Iijima H, Aoki T, et al. Usefulness of liver fibrosis markers ELF in chronic hepatitis. Kanzo 2015; 56 (10): 543-5.
19) Yamazaki T, Joshita S, Umemura T, et al. Association of serum autotaxin levels with liver fibrosis in patients with chronic hepatitis c. Sci Rep 2017; 7: 46705.
20) Parkes J, Guha IN, Roderick P, et al. Enhanced liver fibrosis (ELF) test accurately identifies liver fibrosis in patients with chronic hepatitis C. J Viral Hepat 2011; 18 (1): 23-31.
21) Mayo MJ, Parkes J, Adams-Huet B, et al. Prediction of clinical outcomes in primary biliary cirrhosis by serum enhanced liver fibrosis assay. Hepatology 2008; 48 (5): 1549-57.
22) Nobili V, Parkes J, Bottazzo G, et al. Performance of ELF serum markers in predicting fibrosis stage in pediatric non-alcoholic fatty liver disease. Gastroenterology 2009; 136 (1): 160-7.
23) Hur M, Park M, Moon HW, et al. Comparison of non-invasive clinical algorithms for liver fibrosis in patients with chronic hepatitis B to reduce the need for liver biopsy: application of enhanced liver fibrosis and Mac-2 binding protein glycosylation isomer. Ann Lab Med 2022; 42 (2): 249-57.

Original

A prospective evaluation of Roche's newly developed SARS-CoV-2 Rapid Antigen Test 2.0 using anterior nasal and nasopharyngeal specimens

†Yusaku Akashi, MD, PhD[1,2,3], Michiko Horie*[4], Chisako Yamada*[5], Yuto Takeuchi*[2,6], Atsuo Ueda*[7], Shigeyuki Notake*[7], Koji Nakamura*[7], Norihiko Terada*[6], Yoko Kurihara*[6], Hiromichi Suzuki*[1,2,6]*

†Corresponding author: Division of Infectious Diseases, Department of Medicine, Tsukuba Medical Center Hospital, 1-3-1 Amakubo Tsukuba, Ibaraki 305-8558, Japan.
E-mail: yusaku-akashi@umin.ac.jp
Received April 17, 2024; accepted September 6, 2024
*1 Department of Infectious Diseases, Faculty of Medicine, University of Tsukuba, 1-1-1 Tennodai, Tsukuba, Ibaraki 305-8575, Japan
*2 Division of Infectious Diseases, Department of Medicine, Tsukuba Medical Center Hospital, 1-3-1 Amakubo Tsukuba, Ibaraki 305-8558, Japan
*3 Akashi Internal Medicine Clinic, 3-1-63 Asahigaoka, Kashiwara, Osaka 582-0026, Japan
*4 Roche Diagnostics K.K, Medical Scientific Affairs Group, Shinagawa Season Terrace 1-2-70, Konan, Minato-ku, Tokyo, 108-0075, Japan
*5 Roche Diagnostics K.K, Customer Care Group, Shinagawa Season Terrace 1-2-70, Konan, Minato-ku, Tokyo, 108-0075, Japan
*6 Department of Infectious Diseases, University of Tsukuba Hospital, 2-1-1 Amakubo, Tsukuba, Ibaraki 305-8576, Japan
*7 Department of Clinical Laboratory, Tsukuba Medical Center Hospital, 1-3-1 Amakubo, Tsukuba, Ibaraki 305-8558, Japan

ABSTRACT

Rapid qualitative antigen tests are essential for the management of COVID-19, but their sensitivity and specificity vary. This study prospectively evaluated the diagnostic performance of a newly developed product, the SARS-CoV-2 Rapid antigen test 2.0 (Roche Diagnostics GmbH, Mannheim, Germany) in anterior nasal and nasopharyngeal samples, comparing results with reverse transcription polymerase chain reaction (RT-PCR) in nasopharyngeal samples. The symptomatic participants or asymptomatic participants with a history of close contact with COVID-19 patients were consecutively enrolled. The study also evaluated the sensitivities across different viral loads in pooled samples with known viral RNA levels and compared them with those of a previous product.

Among 287 participants, 283 were symptomatic and 187 tested positive for SARS-CoV-2; 179 nasopharyngeal samples had viral loads ≥ 1,000 copies/test. The antigen test had a sensitivity of 92.5% (95% confidence interval [CI] : 87.8%-95.8%) and specificity of 100% (95% CI: 96.4%-100%) in anterior nasal samples. When stratified by viral loads in the corresponding nasopharyngeal samples (≥ 10^5, ≥ 10^4 to <10^5 , ≥ 10^3 to <10^4, ≥ 10^2 to <10^3, and <10^2 viral copies/test), the sensitivities were 95.9%, 91.3%, 70.0%, 100%, and 40%, respectively. For nasopharyngeal samples, the sensitivity and specificity of the antigen test were 97.3% (95% CI: 93.9%-99.1%) and 99.0% (95% CI: 94.6%-100%), respectively. In the evaluation of pooled samples, the SARS-CoV-2 Rapid antigen test 2.0 demonstrated a lower limit of detection for SARS-CoV-2 compared to the previous product.

The SARS-CoV-2 Rapid antigen test 2.0 exhibited sufficient diagnostic performance, with improved detection performance over the previous products.

〔Lab Med Int 2025; 4 (1) : 21-28〕

Key Words
lateral flow qualitative antigen testing, COVID-19, nasal and nasopharyngeal samples, Point-of-Care testing, SARS-CoV-2 Rapid antigen test 2.0

I. INTRODUCTION

Severe acute respiratory syndrome coronavirus-2 (SARS-CoV-2) has been prevailing and causing coronavirus disease (COVID-19) worldwide [1]. Despite advancements in treatments and vaccination efforts, COVID-19 continues to pose a significant health threat to vulnerable populations [1], underscoring the critical need for prompt and accurate diagnosis for effective infection control. While molecular examinations are the gold standard for COVID-19 diagnosis because of their high reliability [2], rapid antigen tests have been widely used due to their convenience, immediate results, and wide availability [3].

Prior to the emergence of the Omicron variant and other subsequent variants, the SARS-CoV-2 Rapid antigen test (Roche Diagnostics GmbH, Mannheim, Germany) showed sufficient sensitivity and specificity in nasopharyngeal samples [4]. However, our previous study revealed a significant decrease in the test's sensitivity for samples containing low viral load, e.g., anterior nasal samples [4]. As such, re-evaluating and improving the diagnostic performance of this product seem warranted.

The SARS-CoV-2 Rapid antigen test 2.0 (Roche Diagnostics GmbH, Mannheim, Germany) is an improved version of the SARS-CoV-2 Rapid antigen test using new reagents but its utility with clinical samples has not yet been evaluated. In this study, we conducted a prospective evaluation of the diagnostic performance of the SARS-CoV-2 Rapid antigen test 2.0 using both anterior nasal and nasopharyngeal samples. Additionally, we assessed its sensitivity across a range of viral loads by analyzing pooled samples with known quantities of viral RNA.

II. MATERIALS AND METHODS

The evaluations were performed at a drive-through PCR center in Tsukuba Medical Center Hospital (TMCH; Tsukuba, Japan) between August 16 and August 29, 2022. All of the participants were referred for SARS-CoV-2 RT-PCR from 42 clinics and a local public health center as previously described [5][6]. The study included participants having symptoms compatible with COVID-19 or a history of close contact with COVID-19 patients if they were asymptomatic. The results of the SARS-CoV-2 Rapid antigen test 2.0 were compared with those of RT-PCR with nasopharyngeal samples. One anterior nasal sample and two nasopharyngeal samples were simultaneously collected from participants after obtaining their verbal informed consent. The informed consent process was performed verbally to prevent infection transmission and was documented in the corresponding electronic medical record. The ethics board of the University of Tsukuba approved the protocol (approval number: R03-041).

Sample collection and antigen testing with SARS-CoV-2 Rapid antigen test 2.0

Anterior nasal samples were first obtained from both nostrils, as previously described [4], and two nasopharyngeal samples were then collected for antigen testing and RT-PCR following the recommended procedure [7]. The swab included in the antigen test kits was used for antigen testing, and a FLOQSwab (Copan ItaliaSpA, Brescia, Italy) was used for RT-PCR. All sample collections were performed by trained medical staff. Antigen testing was performed immediately after sample collection.

Procedures for RT-PCR examinations

For RT-PCR, swabs collected from the nasopharynx were suspended in 3 mL of Universal Transport Medium (UTM; Copan Italia SpA) and preserved at −80℃ after in-house RT-PCR at the TMCH microbiology department. The in-house RT-PCR was performed primarily for clinical purposes and its procedures for in-house RT-PCR have been described previously [8][9]. Briefly, purification and RNA extraction were performed using a magLEAD 6gC (Precision System Science Co., Ltd., Chiba, Japan) from 200 μL aliquots of UTM. The GENECUBE® (TOYOBO Co., Ltd., Osaka, Japan) and GENECUBE® HQ SARS-CoV-2 assays, which target the N region, were used for detecting SARS-CoV-2. The UTM was then transported to LSI Medience Corporation (Tokyo, Japan) for reference RT-PCR testing.

As a reference, real-time RT-PCR at LSI Medience Corporation was performed using the national standard method developed by the National Institute of Infectious Diseases (NIID), Japan [5][10]–[13]. The purification and RNA extraction were performed on 200-μL aliquots of UTM samples using the Maxwell® RSC Viral Total Nucleic Acid Purification Kit and Maxwell® RSC 48 Instrument (Promega Corporation, Madison, WI, USA). The NIID test targets the N2 region, and the RT-PCR equipment included the cobas® z480 (Roche Diagnostics International Ltd., Rotkreuz, Switzerland), the QuantiTect®

Probe RT-PCR Kit (QIAGEN, Hilden, Germany), and a SARS-CoV-2 standard (Exact Diagnostics LLC, Fort Worth, TX, USA). Viral loads were quantified using the NIID N2 method with calibration curves generated from EDX SARS-CoV-2 Standard (Bio-Rad Laboratories, Inc., Hercules, CA, USA) at concentrations of 100, 125, 250, 500, and 1000 copies/reaction. The average viral load of the duplicate assays per sample was used for analysis.

Samples with discrepancies between in-house RT-PCR and NIID N2 RT-PCR underwent further testing using the cobas® Liat® system and cobas® Liat SARS-CoV-2 & Influenza A/B (Liat; Roche Molecular Systems, Inc., Pleasanton, CA, USA)[14)–16)]. The Liat assays were exclusively used for resoloving the discordance, with their results considered definitive for determining the SARS-CoV-2 status of the sample.

Evaluation of limit of detection of the SARS-CoV-2 Rapid antigen test 2.0 and the SARS-CoV-2 Rapid antigen test

To evaluate the limit of detection (LOD) for SARS-CoV-2 using the SARS-CoV-2 Rapid antigen test 2.0, we prepared samples of 7 concentrations for the evaluation by serially diluting 4 pooled positive samples with 5 negative matrix samples (UTM; four pooled nasopharyngeal samples). The 4 pooled positive samples were prepared from preserved UTM media of participants previously diagnosed with COVID-19.

For each concentration, 20 samples were prepared, resulting in a total of 140 samples for the study. The LOD evaluation was performed concurrently with the SARS-CoV-2 Rapid antigen test 2.0 and the SARS-CoV-2 Rapid antigen test.

For antigen testing with both kits, 350 μL of each of the 140 specimens were added with an equal volume of the extraction buffer provided in the antigen kit. The antigen tests were performed following the manufacturer's instructions, and the interpretation of the antigen test results was carried out by two independent medical technicians in a blinded manner. To ensure blinding, all samples were randomly numbered by other researchers before being provided to the technicians. The limit of detection (LOD) was defined as the viral concentration at which both examiners achieved a detection sensitivity of >95%.

Statistical analyses

The sensitivity and specificity of the antigen tests were calculated with 95% confidence intervals (CIs). The sensitivity was stratified according to the viral loads assessed by the N2 set of the NIID method. If a sample had tested negative on the NIID N2 RT-PCR but positive on the in-house RT-PCR and Liat assay, it would have been considered to have a minimal viral load of < 100 copies/test.

All statistical analyses were conducted using the R 4.1.2 software program (R Foundation, Vienna, Austria) with the "readxl," "tidyverse," and "epiR" packages.

III. RESULTS

In this study, 287 participants were assessed, and 283 (98.6%) were found to be symptomatic. The median interval from symptom onset to sample collection was 1.0 days (IQR: 1.0-2.0 days). The NIID N2 assays were positive in 185 samples and negative in 102 samples, among which the results of 5 samples were different from those of in-house RT-PCR tests. Of the 5 samples, the Liat assays were positive in 3 and negative in 2 (**Supplementary Table 1**). As a result, we considered SARS-CoV-2 to be positive in 187 (65.2%) and negative in 100 samples (34.8%).

Diagnostic performance of SARS-CoV-2 Rapid antigen test 2.0 in anterior nasal samples

Table 1 shows the diagnostic performance of SARS-CoV-2 Rapid antigen test 2.0 in anterior nasal samples. The overall sensitivity and specificity were 92.5% (95% CI: 87.8%–95.8%) and 100% (95% CI: 96.4%–100%), respectively. When stratified by viral loads of copies/test (with $\geq 10^5$, $\geq 10^4$ to $<10^5$, $\geq 10^3$ to $<10^4$, $\geq 10^2$ to $<10^3$, and $<10^2$) in the corresponding nasopharyngeal samples, the sensitivities were 95.9% (95% CI: 91.3%–98.5%), 91.3% (95% CI: 72.0%–98.9%), 70.0% (95% CI: 34.8%–93.3%), 100% (29.2%–100%), and 40.0% (95% CI: 0%–84.2%), respectively (**Table 2**).

Diagnostic performance of SARS-CoV-2 Rapid antigen test 2.0 in nasopharyngeal samples

The SARS-CoV-2 Rapid antigen test 2.0 demonstrated an overall sensitivity of 97.3% (95% CI: 93.9–99.1%) and specificity of 99.0% (95% CI: 94.6–100%) when using nasopharyngeal samples (**Table 3**). As shown in **Table 4**, the sensitivities of the SARS-CoV-2 Rapid antigen test 2.0 for nasopharyngeal samples with viral loads of $\geq 10^5$, $\geq 10^4$ to $<10^5$, $\geq 10^3$ to $<10^4$, $\geq 10^2$ to $<10^3$, and $<10^2$ copies/test were 99.3% (95% CI: 96.2–100%), 100% (95% CI: 85.2–100%), 90.0% (95% CI: 55.5–99.7%), 100% (95% CI: 29.2–100%), and 40% (95% CI: 5.3–85.3%), respectively.

Table 5 summarizes the variation in sensitivity of the SARS-CoV-2 Rapid antigen test 2.0 according to days

since symptom onset. While sensitivity in anterior nasal samples increased from 86.7% on day 0 to 100% from day 3 onwards, nasopharyngeal samples consistently demonstrated a sensitivity exceeding 90% throughout the observation period.

Evaluation and comparison of the limit of detection of the SARS-CoV-2 Rapid antigen test 2.0 and the SARS-CoV-2 Rapid antigen test

For the SARS-CoV-2 Rapid antigen test 2.0, both investigators reported 100% detection rates at concentrations of 6,250 copies/test and higher on the corresponding UTM samples (**Table 6**). In contrast, for the SARS-CoV-2 Rapid antigen test, both investigators demonstrated 100% detection rates up to a concentration of 12,500 copies/test. The complete dataset was provided as Supplementary **Table 2**.

IV. DISCUSSION

Among anterior nasal and nasopharyngeal samples, the SARS-CoV-2 Rapid antigen test 2.0 demonstrated high sensitivities of 92.5% and 97.3%, retaining specificities

Table 1 Diagnostic performance of the SARS-CoV-2 Rapid antigen test 2.0 with anterior nasal samples

		Real-time RT-PCR	
		Positive	Negative
Antigen test	Positive	173	0
	Negative	14	100
Sensitivity (%)		92.5 (87.8–95.8)	
Specificity (%)		100 (96.4–100)	

RT-PCR, reverse transcription-polymerase chain reaction
Data in parentheses indicate 95% confidence intervals.

Table 2 Sensitivity of the SARS-CoV-2 Rapid antigen test 2.0 with anterior nasal samples stratified by viral loads of RT-PCR with nasopharyngeal samples

Virus copies/test (NIID, N2)	Sensitivity (%)	Positive	Negative
$\geq 10^5$	95.9 (91.3–98.5)	140	6
10^4–10^5	91.3 (72.0–98.9)	21	2
10^3–10^4	70.0 (34.8–93.3)	7	3
10^2–10^3	100 (29.2–100)	3	0
$< 10^2$	40 (5.3–85.3)	2*	3*

NIID, National Institute of Infectious Diseases (NIID), Japan; RT-PCR, reverse transcription-polymerase chain reaction
* The viral loads of three SARS-CoV-2 positive samples, which tested negative on the NIID N2 assay but positive on both the in-house PCR and Liat assay, were determined to be below 100 copies/test.
Data in parentheses indicate 95% confidence intervals.
The viral loads for RT-PCR were determined using the NIID (N2 gene), Japan method

Table 3 Diagnostic performance of the SARS-CoV-2 Rapid antigen test 2.0 with nasopharyngeal samples

		Real-time RT-PCR	
		Positive	Negative
Antigen test	Positive	182	1
	Negative	5	99
Sensitivity (%)		97.3 (93.9–99.1)	
Specificity (%)		99.0 (94.6–100)	

RT-PCR, reverse transcription-polymerase chain reaction
Data in parentheses indicate 95% confidence intervals.

Table 4 Sensitivity of the SARS-CoV-2 Rapid antigen test 2.0 with nasopharyngeal samples stratified by viral loads of RT-PCR with nasopharyngeal samples

Virus copies/test (NIID, N2)	Sensitivity (%)	Positive	Negative
$\geq 10^5$	99.3 (96.2–100)	145	1
10^4–10^5	100 (85.2–100)	23	0
10^3–10^4	90.0 (55.5–99.7)	9	1
10^2–10^3	100 (29.2–100)	3	0
$< 10^2$	40 (5.3–85.3)	2*	3*

NIID, National Institute of Infectious Diseases (NIID), Japan; RT-PCR, reverse transcription-polymerase chain reaction

* The viral loads of three SARS-CoV-2 positive samples, which tested negative on the NIID N2 assay but positive on both the in-house PCR and Liat assay, were determined to be below 100 copies/test.

Data in parentheses indicate 95% confidence intervals.

The viral loads for RT-PCR were determined using the NIID (N2 gene), Japan method

Table 5 Sensitivity of the SARS-CoV-2 Rapid antigen test 2.0 stratified by the number of days since symptom onset

Anterior nasal samples			
Days since onset	Sensitivity (%)	Positive	Negative
0	86.7 (59.5–98.3)	13	2
1	86.9 (77.8–93.3)	73	11
2	97.8 (88.5–99.9)	45	1
3	100 (82.4–100)	19	0
4	100 (69.2–100)	10	0
>5	100 (54.1–100)	6	0
Nasopharyngeal samples			
Days since onset	Sensitivity (%)	Positive	Negative
0	100 (78.2–100)	15	0
1	95.2 (88.3–98.7)	80	4
2	100 (92.3–100)	46	0
3	94.7 (74.0–99.9)	18	1
4	100 (69.2–100)	10	0
>5	100 (54.1–100)	6	0

Of the 283 symptomatic participants included in the data, onset date was unavailable for 11.

Data in parentheses indicate 95% confidence intervals.

Table 6 Detection rates of SARS-CoV-2 Rapid antigen test 2.0 and SARS-CoV-2 Rapid antigen test at different viral concentrations using pooled positive samples

Viral Concentration on UTM samples (copies/test)	SARS-CoV-2 Rapid antigen test 2.0		SARS-CoV-2 Rapid antigen test	
	Examiner A	Examiner B	Examiner A	Examiner B
100,000	100% (20/20)	100% (20/20)	100% (20/20)	100% (20/20)
50,000	100% (20/20)	100% (20/20)	100% (20/20)	100% (20/20)
25,000	100% (20/20)	100% (20/20)	100% (20/20)	100% (20/20)
12,500	100% (20/20)	100% (20/20)	100% (20/20)	100% (20/20)
6,250	100% (20/20)	100% (20/20)	90% (18/20)	100% (20/20)
3,125	95% (19/20)	90% (18/20)	75% (15/20)	65% (13/20)
1,563	55% (11/20)	50% (10/20)	35% (7/20)	25% (5/20)

UTM, Universal Transport Medium

The values in parentheses represent the number of positive samples detected out of the total number of samples tested at each concentration.

of 100% and 99.0%, respectively. In addition, the analysis of pooled positive samples in this study also suggested a lower LOD of SARS-CoV-2 Rapid antigen test 2.0 compared to its previous product.

The anterior nostrils generally have a lower viral load than the nasopharynx [17]. In fact, according to our previous study, the SARS-CoV-2 Rapid antigen test showed a modest sensitivity of 72.7% in anterior nasal samples [4]. However, in the current study, the diagnostic performance of the SARS-CoV-2 Rapid antigen test 2.0 was high and comparable for both sample types. A notable difference in sensitivity existed only in samples with viral loads of 103–104 copies/test, with sensitivities of 70.0% and 90.0% for anterior nasal and nasopharyngeal samples, respectively (**Table 2 and Table 4**). This finding suggests that the sensitivity of the current product has improved compared to the SARS-CoV-2 Rapid antigen test. In addition, our pooled sample analysis, which showed a better LOD for the SARS-CoV-2 Rapid antigen test 2.0 than for the original SARS-CoV-2 Rapid antigen test, provides further evidence of its improved sensitivity.

The high sensitivity of the SARS-CoV-2 Rapid antigen test 2.0 in anterior nasal samples can increase the utility of antigen tests. Anterior nasal sample collections may prevent the induction of cough or sneezing during sample collection, thus reducing virus transmission from patients [18]. In addition, anterior nasal sample collection is less burdensome and more suitable for self-testing than nasopharyngeal collection [19]. Despite showing a slight decrease in sensitivity on the first and following days of symptom onset (**Table 5**), the SARS-CoV-2 Rapid antigen test 2.0 maintains good performance with anterior nasal samples. The availability of several antigen tests as over-the-counter products has contributed to the increasing popularity and widespread use of self-testing. The good sensitivity of the SARS-CoV-2 Rapid antigen test 2.0 in anterior nasal samples may further promote the adoption of this sampling method, making testing more accessible and convenient for the general population.

Differences in genome variants of SARS-CoV-2 are another factor that can influence the diagnostic performance of antigen tests. The study period during which this evaluation was performed was the "7th wave" of COVID-19 in Japan, where the Omicron BA4/5 variant was dominant. Compared to the Omicron BA.1 variant, Roche's previous product, SARS-CoV-2 Rapid antigen test, showed a reduced sensitivity for the BA.2, BA.5 variant [20]. Despite this, the SARS-CoV-2 Rapid antigen test 2.0 demonstrated adequate analytical performance with both anterior nasal and nasopharyngeal samples, although the current study did not analyze the genome variant. It is important to note that the diagnostic performance of antigen tests can change with the emergence of other variants and should be continuously evaluated.

Several limitations associated with the present study warrant mention. First, the study population consisted primarily of symptomatic participants, with the majority of corresponding nasopharyngeal UTM samples containing viral loads greater than 10^4 copies/test. Nevertheless, two previous studies have reported similar sensitivities for this antigen test, with 92.9% for nasal samples [21] and 92.1-92.9% for nasopharyngeal samples [21,22], which are consistent with our findings. Second, the use of frozen samples may have influenced the reference test results. Third, the study did not evaluate the potential impact of vaccination status or medication use on the diagnostic performance of the test. Finally, this study's LOD evaluation used samples stored in UTM, while direct inoculation of sampled swabs into the antigen extraction medium is the standard practice in clinical settings. This may have influenced the tests' performance [23–25] and should be considered when interpreting the results of this study.

In conclusion, this first clinical evaluation of the SARS-CoV-2 Rapid antigen test 2.0 showed a sufficient diagnostic performance with both anterior nasal and nasopharyngeal samples. In addition, the product showed an improvement in its LOD for SARS-CoV-2. These results support the clinical utility of the new product for detecting SARS-CoV-2 and highlight the importance of continuous evaluation and improvement of rapid antigen tests.

ACKNOWLEDGEMENTS

COBAS and LIAT are trademarks of Roche. SARS-CoV-2 Rapid antigen test 2.0 is manufactured by SD Biosensor and distributed by Roche Diagnostics.

AUTHORSHIP CONTRIBUTIONS

All authors meet criteria for authorship set by the International Committee of Medical Journal Editors. Yusaku Akashi was the principal investigator, wrote the first draft of the manuscript, and performed the statistical analyses. Michiko Horie and Hiromichi Suzuki designed the study. Chisako Yamada performed the molecular testing using the cobas® Liat® system and cobas® Liat SARS-CoV-2 & Influenza A/B. Atsuo Ueda, Shigeyuki Notake and Koji Nakamura collected the samples and performed the diagnostic tests. Hiromichi Suzuki supervised the project. All authors contributed to writing the final draft of the manuscript.

DISCLOSURE OF CONFLICT OF INTERESTS

Roche Diagnostics, Co., Ltd financially supported this study and provided remuneration to Michiko Horie and Chisako Yamada. Hiromichi Suzuki received lecture fees from Roche Diagnostics K.K.

REFERENCES

1) World Health Organization. Weekly epidemiological update on COVID-19-5 October 2022. [cited 2022 Oct 10]. Available from: https://www.who.int/publications/m/item/weekly-epidemiological-update-on-covid-19---5-october-2022
2) Centers for Disease Control and Prevention. Nucleic Acid Amplification Tests (NAATs). [cited 2022 Oct 10] Available from: https://www.cdc.gov/coronavirus/2019-ncov/lab/naats.html
3) Centers for Disease Control and Prevention. Guidance for Antigen Testing for SARS-CoV-2 for Healthcare Providers Testing Individuals in the Community. [cited 2022 Oct 11]. Available from: https://stacks.cdc.gov/view/cdc/115045
4) Akashi Y, Horie M, Takeuchi Y, et al. A prospective clinical evaluation of the diagnostic accuracy of the SARS-CoV-2 rapid antigen test using anterior nasal samples. J Infect Chemother 2022; 28 (6): 780-5. doi: 10.1016/j.jiac.2022.02.016.
5) Takeuchi Y, Akashi Y, Kiyasu Y, et al. A prospective evaluation of diagnostic performance of a combo rapid antigen test QuickNavi-Flu+COVID19 Ag. J Infect Chemother 2022; 28 (6): 840-3. doi: 10.1016/j.jiac.2022.02.027.
6) Suzuki H, Akashi Y, Kato D, et al. Analytical performance of the rapid qualitative antigen kit for the detection of SARS-CoV-2 during widespread circulation of the Omicron variant. J Infect Chemother 2023; 29 (3): 257-62. doi: 10.1016/j.jiac.2022.11.006.
7) Marty FM, Chen K, Verrill KA. How to Obtain a Nasopharyngeal Swab Specimen. N Engl J Med 2020; 382 (22): e76. doi: 10.1056/NEJMvcm2010260.
8) Naito A, Kiyasu Y, Akashi Y, et al. The evaluation of the utility of the GENECUBE HQ SARS-CoV-2 for anterior nasal samples and saliva samples with a new rapid examination protocol. PLoS One 2021; 16 (12): e0262159. doi: 10.1371/journal.pone.0262159.
9) Kiyasu Y, Akashi Y, Sugiyama A, et al. A Prospective Evaluation of the Analytical Performance of GENECUBE® HQ SARS-CoV-2 and GENECUBE® FLU A/B. Mol Diagn Ther 2021; 25 (4): 495-504. doi: 10.1007/s40291-021-00535-5.
10) Shirato K, Nao N, Katano H, et al. Development of Genetic Diagnostic Methods for Detection for Novel Coronavirus 2019 (nCoV-2019) in Japan. Jpn J Infect Dis. 2020; 73 (4): 304-7. doi: 10.7883/yoken.JJID.2020.061.
11) Akashi Y, Kiyasu Y, Takeuchi Y, et al. Evaluation and clinical implications of the time to a positive results of antigen testing for SARS-CoV-2. J Infect Chemother. 2022; 28 (2): 248-51. doi: 10.1016/j.jiac.2021.10.026.
12) Ishikane M, Unoki-Kubota H, Moriya A, et al. Evaluation of the QIAstat-Dx Respiratory SARS-CoV-2 panel, a rapid multiplex PCR method for the diagnosis of COVID-19. J Infect Chemother 2022; 28 (6): 729-34. doi: 10.1016/j.jiac.2022.02.004.
13) Tsujimoto Y, Terada J, Kimura M, et al. Diagnostic accuracy of nasopharyngeal swab, nasal swab and saliva swab samples for the detection of SARS-CoV-2 using RT-PCR. Infect Dis (Lond). 2021; 53 (8): 581-9. doi: 10.1080/23744235.2021.1903550.
14) Akashi Y, Horie M, Kiyotaki J, et al. Clinical Performance of the cobas Liat SARS-CoV-2 & Influenza A/B Assay in Nasal Samples. Mol Diagn Ther 2022; 26 (3): 323-31. doi: 10.1007/s40291-022-00580-8.
15) Blackall D, Moreno R, Jin J, et al. Performance Characteristics of the Roche Diagnostics cobas Liat PCR System as a COVID-19 Screening Tool for Hospital Admissions in a Regional Health Care Delivery System. J Clin Microbiol. 2021; 59 (10): e0127821. doi: 10.1128/JCM.01278-21.
16) Mahmoud SA, Ganesan S, Ibrahim E, et al. Evaluation of six different rapid methods for nucleic acid detection of SARS-COV-2 virus. J Med Virol 2021; 93 (9): 5538-43. doi: 10.1002/jmv.27090.
17) Zhou Y, O'Leary TJ. Relative sensitivity of anterior nares and nasopharyngeal swabs for initial detection of SARS-CoV-2 in ambulatory patients: Rapid review and meta-analysis. PLoS One 2021; 16 (7): e0254559. doi: 10.1371/journal.pone.0254559.
18) Takeuchi Y, Akashi Y, Kato D, et al. Diagnostic performance and characteristics of anterior nasal collection for the SARS-CoV-2 antigen test: a prospective study. Sci Rep 2021; 11 (1): 10519. doi: 10.1038/s41598-021-90026-8.
19) Waggoner JJ, Vos MB, Tyburski EA, et al. Concordance of SARS-CoV-2 Results in Self-collected Nasal Swabs vs Swabs Collected by Health Care Workers in Children and Adolescents. JAMA 2022; 328 (10): 935-40. doi: 10.1001/jama.2022.14877.
20) Leuzinger K, Roloff T, Egli A, et al. Impact of SARS-CoV-2 Omicron on Rapid Antigen Testing Developed for Early-Pandemic SARS-CoV-2 Variants. Microbiol Spectr 2022; 10 (4): e0200622. doi: 10.1128/spectrum.02006-22.
21) Widyasari K, Kim S. Efficacy of novel SARS-CoV-2 rapid antigen tests in the era of omicron outbreak. PLoS One. 2023; 18 (8): e0289990. doi: 10.1371/journal.pone.0289990.
22) Flinck H, Aittoniemi J. Evaluation of the new 2.0 version of the Roche SARS-CoV-2 Rapid Antigen Test. J Virol Methods 2023; 319: 114758. doi: 10.1016/j.jviromet.2023.114758.
23) Takeuchi Y, Akashi Y, Kato D, et al. The evaluation of a

newly developed antigen test (QuickNavi™-COVID19 Ag) for SARS-CoV-2: A prospective observational study in Japan. J Infect Chemother 2021; 27 (6) : 890-4. doi: 10.1016/j.jiac.2021.02.029.

24) Kiyasu Y, Takeuchi Y, Akashi Y, et al. Prospective analytical performance evaluation of the QuickNavi™-COVID19 Ag for asymptomatic individuals. J Infect Chemother 2021; 27 (10) : 1489-92. doi: 10.1016/j.jiac.2021.07.005

25) Yamayoshi S, Sakai-Tagawa Y, Koga M, et al. Comparison of Rapid Antigen Tests for COVID-19. Viruses 2020; 12 (12) : 1420. doi: 10.3390/v12121420.

Original

GPIHBP1 and Lipoprotein Lipase Level During Pregnancy

*†Hisanobu Sadakata*1, Kazuya Miyashita*2, Yukio Kajita*3, Katsuyuki Nakajima*4, Issei Kagami*5, Yumiko Abe*6, Masami Murakami*7*

†Corresponding author: Tatebayashi Health and Welfare office
E-mail: syaba1969kun@gmail.com
Received July 13, 2024; accepted September 10, 2024
*1 Tatebayashi Health and Welfare office
*2 Immuno-biological Laboratories, Co. Ltd.
*3 Department of Clinical Laboratory, Kiryu Kosei General Hospital
*4 Takasaki University of Health and Welfare
*5 Obsteterics and Gynocology, Kiryu Kosei General Hospital
*6 Gunma University of Health and Welfare, Department of Technology and Clinical Engineering
*7 Gunma University Graduate School of Medicine, Department of Clinical Laboratory Medicine

ABSTRACT

Objective: During pregnancy, lipid metabolism is characterized by accumulation of fats during the first half of pregnancy and an increase in catabolism during the later stages. However, the underlying mechanisms for this shift are not well understood. We attempted to clarify the involvement of glycosylphosphatidylinositol-anchored high-density lipoprotein-binding protein 1 (GPIHBP-1), an anchor protein for lipoprotein lipase (LPL), which is a major lipid metabolism enzyme, by measuring its blood levels during pregnancy.
Methods: Blood samples were collected from non-pregnant women and from pregnant women at different stages: early pregnancy (up to 20 weeks of gestation), mid-pregnancy (21–33 weeks of gestation), late pregnancy (34–41 weeks of gestation), and puerperium (4–8 weeks after delivery). The levels of LPL and GPIHBP-1 were measured in each sample. In addition, these values were adjusted for albumin concentration to account for the effects of physiological blood dilution due to pregnancy.
Results: During pregnancy, GPIHBP-1 and LPL blood concentrations decreased transiently but returned to non-pregnant levels after delivery. When adjusted for albumin concentration, the decrease in GPIHBP-1 levels was negated, while the decrease of LPL levels was preserved.
Conclusions: During the course of normal pregnancy, the levels of GPIHBP-1 showed a transient decrease, which was thought to be due to physiological dilution. The levels of blood LPL also showed transient decrease probably due to inhibition of lipolysis.

〔Lab Med Int 2025; 4 (1) : 29-33〕

Key Words
lipid metabolism, lipoprotein lipase, physiological changes, pregnant women

I. Introduction

Blood triglyceride levels are known to be increased in patients with diabetes mellitus and severe obesity. It is believed that suppression of lipolytic enzymes, which are normally regulated by insulin in healthy individuals, has been the mechanism for this increase. In patients with increased insulin resistance, the control exerted by insulin is weakened, resulting in an accumulation of triglycerides that remain unmetabolized.

Lipoprotein lipase (LPL) is an enzyme responsible for degrading lipoproteins, while glycosylphosphatidylinosi-

tol-anchored high-density lipoprotein-binding protein 1 (GPIHBP1) serves as a critical scaffold for LPL on the vascular endothelium.

Lipids absorbed through the intestine are present in the blood as lipoproteins, which are complexes of lipids and proteins. To be used as energy, the triglycerides within these lipoproteins must be hydrolyzed to produce free fatty acids. Additionally, lipoproteins are converted into smaller lipoproteins and stored in the liver. LPL and GPIHBP-1 are known to play key roles in these processes [1].

It has been reported that decreased activity or genetic mutations in GPIHBP1 [2,3] and defects in LPL [4] cause abnormal elevations in blood lipid levels.

Moreover, LPL expression is known to be regulated by insulin, and LPL blood levels tend to be low in conditions characterized by insulin resistance or obesity [5].

On the other hand, blood levels of total cholesterol (TC) and triglycerides (TG) are well known to increase as pregnancy progresses through the gestational weeks.

During pregnancy, a characteristic of lipid metabolism is the increased fat assimilation and accumulation in the earlier stages, which is followed by enhanced catabolism of maternal fat in the later stages to satisfy the heightened demand as the fetus grows.

It has been reported that human placental lactogen (hPL), which a hormone derived from the placenta, has an anti-insulin effect that suppresses maternal glucose utilization [6]. Additionally, it plays a role in lipolysis in later stages of pregnancy owing to its lipolytic activity. As mentioned previously, during pregnancy, fat metabolism undergoes unique changes, but the specific alterations in lipolytic enzymes during this process have not been fully clarified.

Therefore, we decided to investigate the levels of blood GPIHBP1 and LPL throughout the course of a normal pregnancy.

II. Materials and Methods

(Subjects)

This study was approved by the Kiryu Kosei Hospital Ethical Review Board for Medical Research Involving Human Subjects.

The subject of this study included pregnant women who underwent pregnancy management at Kiryu Kosei Hospital. Excluded from this study were women with hypertension, diabetes, or endocrine disorders. In addition, women with multiple pregnancies, intrauterine fetal death, smokers, and heavy drinkers were also excluded.

Serum samples were collected from subjects at four different points: early pregnancy (defined in this study as before 20 weeks of gestation), mid-pregnancy (21–33 weeks), late pregnancy (34–41 weeks), and the puerperium (4–8 weeks after birth). During mid-pregnancy, 50 grams of glucose were administered, and blood samples were collected one hour later as a screening for glucose intolerance. Serum samples were collected without any dietary or water restrictions during the other periods.

The samples were stored at −80℃ until the following measurements after routine biochemical analyses at the hospital laboratory.

Serum samples were also collected from non-pregnant women who provided consent to participate in the study.

(Measurements)

GPIHBP-1 was measured by using the sandwich ELISA method using Anti-Human GPIHBP-CH79A4 Rat IgG monoclonal antibody and HRP-conjugated Anti-Human GPIHBP1-HE20A6 rat IgG Fab' as detection antibodies (#27279 Human GPIHBP1 Assay Kit, IBL Co., Ltd, Fujioka, Japan) [7]. The intra-assay coefficients of variation were 1.9%–5.0% and 1.7%–3.0% at 49.8–56.7 ng/L and 218.5–262.3 ng/L, respectively. The inter-assay coefficients of variation were 0.07 and 0.04% at 56.6 ng/L and 234.1 ng/L, respectively.

LPL was also measured by using the sandwich ELISA method using Anti human LPL N3A1 Mouse IgG monoclonal antibody and HRP-conjugated anti-human LPL 88B8 mouse IgG as detection antibody (#27268 Human Lipoprotein Lipase (LPL) Assay Kit, IBL Co., Ltd, Fujioka, Japan) [8].

Blood levels of TG and TC were measured by using the GP-HPLC method (LipoSEARCH®, IBL).

Concentrations of total protein and albumin were measured at LSI Medience.

(Analysis)

Statistical analysis was carried out using the Mann–Whitney U test, and a P-value of <0.05 was considered statistically significant.

III. Results

A total of 67 pregnant women were recruited for the study. However, 11 of them were diagnosed with glucose intolerance during pregnancy and were excluded from the study. Hence, the final group consisted of 56 pregnant women.

The following are the number of blood samples collected at each stage: 29 during early pregnancy, 39 during mid-pregnancy, 47 during late pregnancy, and 17 during the puerperium. 16 blood samples were collected from non-pregnant women.

Table 1 presents the background of the subjects. The

distribution of age and weight was nearly identical between the non-pregnant women group and the pregnant women group.

First, we measured total protein and albumin at each stage of pregnancy as indicators of physiological blood dilution resulting from pregnancy. Total protein levels decreased to 80.6% as expected of those in non-pregnant women during the mid-pregnancy, while albumin levels decreased to 67.3% of those in non-pregnant women during the late pregnancy (**Fig. 1**).

As shown in **Figure 2**, the level of GPIHBP-1 transiently decreased to a statistically significant level during pregnancy; then it recovered to the level seen in non-pregnant women. However, the decrease was only slight and not statistically significant after adjusting for albumin concentration.

On the contrary, the level of LPL showed a statistically significant decrease during late pregnancy transiently, and then it recovered to a level that exceeded that of non-pregnant women, even after adjusting for albumin concentration.

IV. Discussion

The changes in the levels of GPIHBP-1 and LPL during the course of a normal pregnancy were clarified. The levels of GPIHBP-1 showed a transient decrease and then returned to the level observed in non-pregnant women, but this effect was nullified when corrected for albumin levels.

Consequently, it is most likely that this decrease was the result of a dilution caused by increased blood volume during pregnancy. As a result, it is difficult to state that GPIHBP-1 plays a significant role in metabolism of lipids during pregnancy.

Conversely, the levels of LPL transiently decreased during late pregnancy. As already known, as the placenta grows during pregnancy, levels of hPL increase, resulting in increased insulin resistance within the physiological range. The reduction in blood LPL concentration is probably linked to the suppression of lipolysis, similar to the insulin resistance observed in obesity and diabetes.

In the puerperium, the level of LPL/Alb exceeded the level of nonpregnant woman. It is thought that LPL expression increased with the increased demand for lipid utilization associated with breast milk production during the postpartum period.

V. Limitations

・LPL is anchored to the vascular endothelium by proteoglycans and is released into the blood with the admin-

Table 1 Characteristics of the subjects

	non-pregnant women		pregnant women	
n	16		56	
Age (y)	35	(22 - 42)	31	(19 - 42)
Prepregnant BMI (kg/m^2)	21.5	(21.5 - 28.4)	21.6	(17.2 - 37.9)
Number of primigravida			6	(10.7%)
Gestational age at delivery (weeks)			39.4	(36.7 - 41.4)
Body Weight of the newborn (g)			2969	(2044.0 - 3962.0)
Number of cesarean section			6	(10.7%)

Numbers are average (range)

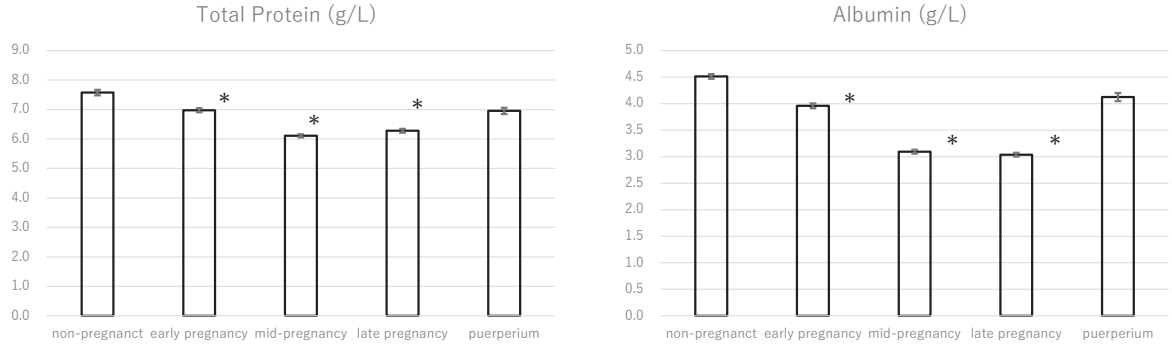

Figure 1 Blood Levels of total protein and albumin

Blood levels of total protein and albumin in non-pregnant women and at each point of pregnancy. Data are presented as average ± standard error. *$p<0.05$ vs. non-pregnant women.

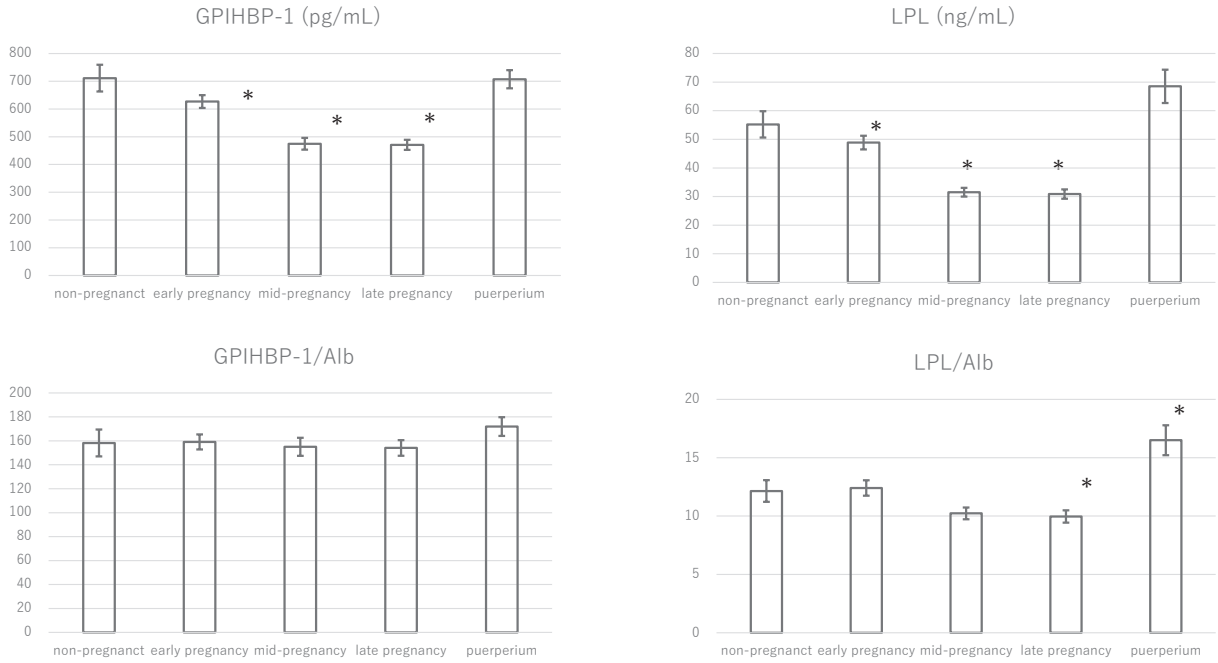

Figure 2 Blood levels of GPIHBP-1 and LPL

The levels of GPIHBP-1 and LPL, both uncorrected and corrected for albumin, in non-pregnant women and at each point of pregnancy. Data are presented as average ± standard error. *p<0.05 vs non-pregnant women.

istration of heparin [8]. In the past, blood samples taken after heparin administration (post-heparin) has been used to measure the level of LPL. However, in recent years, there have been reports indicating that LPL can be adequately assessed even from blood samples without heparin administration (pre-heparin) [9][10].

Since administering heparin to pregnant women is not advisable, it was not done in this study. Although blood samples were collected without the administration of heparin, we think that the measured LPL protein level reflects LPL expression.

・Blood samples were collected without any dietary or water restrictions, except for those from mid-pregnancy, which resulted in significant variations in the time since feeding. The reliability of the data can be affected by these variations.

・Only the blood samples from mid-pregnancy were taken after glucose loading. While there are no reports indicating that glucose loading affects lipid-metabolizing enzymes, the possibility cannot be entirely ruled out.

VI. Conclusion

During the course of normal pregnancy, the levels of blood GPIHBP-1 showed transient decrease to statistically dominant levels, but the decrease was believed to be due to physiological blood dilution that occurs during pregnancy. The levels of blood LPL also showed transient decrease probably due to inhibition of lipolysis.

Authorship Contribution

H.Sadakata, K.Nakajima, I.Kagami and Y.Abe designed the research.

K.Miyashita carried out the measurement of the data.

Y.Kajita collected the samples.

H.Sadakata analysed the data.

M.Murakami made critical reading.

All authors read and approved the final version of the paper.

Disclosure of Conflicts of Interest

The Authors declare that they have no conflict of interest

References

1) Beigneux AP, Miyashita K, Ploug M, et al. Autoantibodies against GPIHBP1 as a Cause of Hypertriglyceridemia. N Engl J Med 2017; 376 (17) : 1647-58. doi: 10.1056/NEJMoa1611930.

2) Rabacchi C, D'Addato S, Palmisano S, et al. Clinical and genetic features of 3 patients with familial chylomicronemia due to mutations in GPIHBP1 gene. J Clin Lipidol 2016; 10 (4) : 915-21.e4. doi: 10.1016/j.jacl.2016.03.009.

3) Rios JJ, Shastry S, Jasso J, et al. Deletion of GPIHBP1 causing severe chylomicronemia. J Inherit Metab Dis 2012; 35 (3) : 531-40. doi:10.1007/s10545-011-9406-5.

4) Wang H, Eckel RH. Lipoprotein lipase: from gene to obesity. Am J Physiol Endocrinol Metab 2009; 297 (2) : E271-88. doi: 10.1152/ajpendo.90920.2008.
5) Hanyu O, Miida T, Obayashi K, et al. Lipoprotein lipase (LPL) mass in preheparin serum reflects insulin sensitivity. Atherosclerosis 2004; 174 (2) : 385-90. doi: 10.1016/j.atherosclerosis.2004.01.034.
6) Handwerger S. Clinical counterpoint: the physiology of placental lactogen in human pregnancy. Endocr Rev. 1991; 12 (4) : 329-36.
7) Hu X, Sleeman MW, Miyashita K, et al. Monoclonal antibodies that bind to the Ly6 domain of GPIHBP1 abolish the binding of LPL. J Lipid Res 2017; 58 (1) : 208-15. doi: 10.1194/jlr.M072462.
8) Miyashita K, Kobayashi J, Imamura S, et al. A new enzyme-linked immunosorbent assay system for human hepatic triglyceride lipase. Clin Chim Acta 2013; 424: 201-6. doi: 10.1016/j.cca.2013.06.016.
9) Kobayashi J. Pre-heparin lipoprotein lipase mass. J Atheroscler Thromb 2004; 11 (1) : 1-5. doi: 10.5551/jat.11.1.
10) Shirakawa T, Nakajima K, Shimomura Y, et al. Comparison of the effect of post-heparin and pre-heparin lipoprotein lipase and hepatic triglyceride lipase on remnant lipoprotein metabolism. Clin Chim Acta 2015; 440: 193-200. doi: 10.1016/j.cca.2014.07.020.

Original

Clinico-laboratory and histological characteristics in patients with gelatinous transformation of bone marrow

Sarina Takeuchi[*1], Mayuko Ichimura Shimizu*[*2], Satoshi Sumida*[*2],*
Koichi Tsuneyama[*2], Mai Kanai*[*3], Shunsuke Watanabe*[*4],*
Takahiko Kasai[*4], †Michiko Yamashita*[*3]*

†Correspondence: Department of Analytical Pathology, Graduate School of Biomedical Sciences, Tokushima University, 3-18-15, Kuramoto-cho, Tokushima-city, Tokushima 770-8503, Japan.
E-mail: yamashitar@tokushima-u.ac.jp
Received February 27, 2024; accepted December 9, 2024
*1 Department of Diagnostic Pathology, Tokushima Prefectural Central Hospital, 1-10-3, Kuramoto-cho, Tokushima-city, Tokushima 770-8539, Japan
*2 Department of Pathology and Laboratory Medicine. Graduate School of Biomedical Sciences, Tokushima University, 3-18-15, Kuramoto-cho, Tokushima-city, Tokushima 770-8503, Japan
*3 Department of Analytical Pathology, Graduate School of Biomedical Sciences, Tokushima University, 3-18-15, Kuramoto-cho, Tokushima-city, Tokushima 770-8503, Japan
*4 Department of Diagnostic Pathology, Japanese Red Cross Tokushima Hospital, 103, Irinokuchi, Komatsushima-cho, Komatsushima-city, Tokushima 773-8502, Japan

ABSTRACT

Gelatinous transformation (GT) is morphological change of fat tissue that reflects malnutrition. In bone marrow with GT, gelatinous deposits occupying hematopoietic space result in hypocellularity. Therefore, GT is presumed to be a cause of secondary anaemia. To characterise clinical feature, laboratory data and histology in patients with bone marrow GT, we enrolled 104 patients who were autopsied at Tokushima University Hospital and Tokushima Red Cross Hospital between August 2015 and July 2020. The patients were aged 71.7 ± 11.4 years (69.2% male individuals). Fifty-eight patients (55.8%) had malignant disease. Bone marrow and liver steatosis and medical records were retrospectively studied. Clinical data and basic blood and urine parameters prior to 3 weeks before death were analysed. Eighteen (17%) patients were assigned to the GT group. In this group, two (11.1%) cases were complicated by bone marrow fibrosis. Immunohistochemically, C-X-C motif chemokine ligand 12 (CXCL12) -positive stromal cells were present in the GT marrow area; however, the number of stellate-shaped reticular cells with projections strongly positive for CXCL12 was reduced. Statistically, GT was not associated with malignant disease, liver fibrosis, or steatosis. In the GT group, serum creatinine was significantly lower than that in the non-GT group (median 0.75 mg/dL, IQR 0.61–1.17, $p=0.047$). The body mass index and geriatric nutritional risk index were also significantly lower in the GT group (median 18.6, IQR 17.3–19.9, $p<0.001$; median 66.8, IQR 61.9–70.6, $p=0.002$, respectively). These results suggest that bone marrow GT indicates protein-energy malnutrition with muscle loss, but not with anaemia.

〔Lab Med Int 2025; 4(1): 34-45〕

Key Words
gelatinous transformation, serum creatinine, bone marrow

I. Introduction

Gelatinous transformation (GT) is known as a representative histologic finding related to malnutrition.[1)–3)] Synonyms for GT include "gelatinous degeneration" and "serous atrophy."[4)] Bone marrow with significant GT is called "gelatinous marrow" or "starvation marrow." In GT of the bone marrow, mucopolysaccharides rich in hyaluronic acid deposit around the fat cells and make the hematopoietic space narrow, leading to hypocellularity; therefore, GT is believed to be a finding of secondary anaemia.

In 2000, Böhm[3)] examined the underlying diseases in 155 cases of GT and identified the following causes: tumours (including hematologic malignancies and carcinomas), malnutrition (including alcoholism and anorexia nervosa), infections (including AIDS and active fevers), maldigestion (including stomach ulcers and post-gastrectomy), heart failure, metabolic disorders (including diabetes mellitus and hypothyroidism), and others. Weight loss or cachexia was found in 78% of the patients and 82% were anaemic. Böhm[3)] concluded that GT represents an indicator of severe illness in patients and that basic bioregulatory processes play a role in its pathogenesis.

However, most bone marrow examinations are performed in the presence of abnormal blood cell counts; thus, investigations using surgical material may have a bias towards anaemia. Many studies that consider anaemia as the basis for GT have been published;[3)5)6)] however, the correlation between GT and anaemia remains controversial.

The purpose of this study is to clarify the relationship between GT and organ failure and the type of PEM by retrospective observation. We also examined the status of hematopoiesis associated mesenchymal cells in GT bone marrow by immunostaining.

II. Materials and Methods

2. 1. Participants

Of the 205 patients who underwent autopsies at Tokushima University Hospital and Tokushima Red Cross Hospital between August 2015 and July 2020, 104 participants aged 18 years or older who had their bone marrow collected were enrolled (**Figure 1**). The enrolled participants' mean age was 71.7 ± 11.4 years and 69.2% were male. Fifty-eight (55.8%) patients had malignant disease, of whom 42 (40.4%) had solid tumours and 16 (15.4%) had haematolymphoid tumours. The exclusion criteria were patients for whom no laboratory data existed 3 weeks before autopsy and pathology specimens could not be prepared due to poor fixation and decalcification. This study was approved by the Ethics Committees of the University of Tokushima Hospital (Application No. 3869-2) and the requirement for informed consent was waived as no personal information was disclosed.

2. 2. Clinical data

Data on height, weight, clinical diagnosis, and autopsy diagnosis of malignancy at the last admission were collected.

3. 3. Laboratory data

Laboratory data 3 weeks before autopsy was obtained. The following blood laboratory parameters were evaluated: white blood cell, total neutrophil, total lymphocyte, red blood cell, and platelet counts; haemoglobin, aspartate aminotransferase, alanine transaminase, alkaline phosphatase, gamma-glutamyl transpeptidase, total bilirubin, total cholesterol, triglyceride, cholinesterase, albumin, total protein, globulin, creatinine, uric acid, and C-reactive protein levels; and the amount of urine protein and occult blood. For each test item, sample size calculation or power analysis was performed. Blood test data were evaluated based on previous studies on reference values for Japanese[7)].

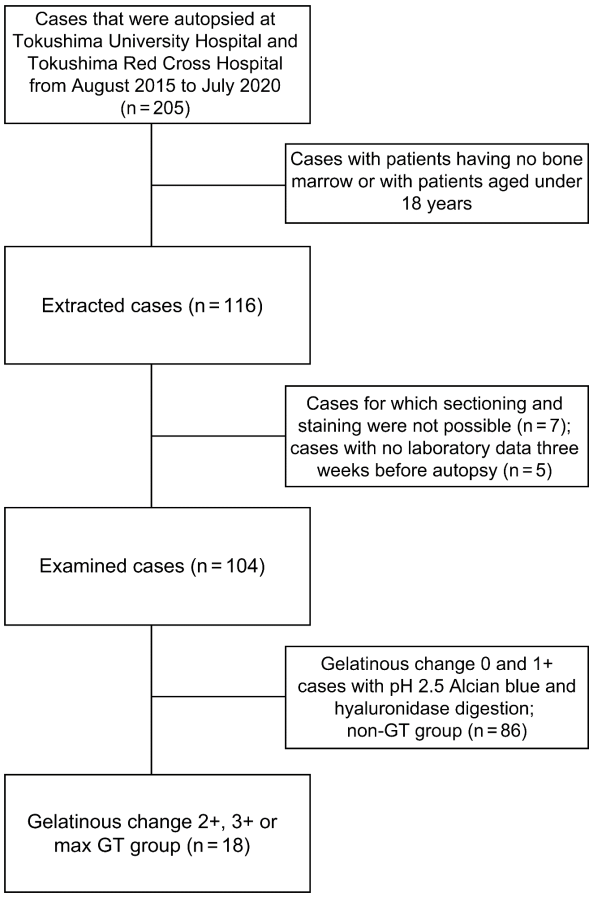

Figure 1 Trial profile. GT, gelatinous transformation.

2. 4. Calculation of nutrition indices

The body mass index (BMI)[8], prognostic nutritional index (PNI)[9], and geriatric nutritional risk index (GNRI)[10] were used as nutritional indices. The calculation formulae are as follows:

BMI = weight (kg)/ [height (m)]^2)

PNI = [10 × serum albumin (g/dL)] + [0.005 × Total lymphocyte count (/mm^3)]

GNRI = [14.89 × serum albumin (g/dL)] + [41.7 × (weight kg / ideal weight kg)]

*Formula for calculating ideal weight:

Male: height (cm)-100-[(height-150)/ 4]

Female: height (cm)-100-[(height-150)/ 2.5]

BMI was evaluated based on previous studies on reference values for Asians[11].

2.5.1 Assessment of bone marrow and liver pathology

Bone marrow specimens were sampled from the L1-2 level vertebra. Ethylenediaminetetraacetic acid decalcification was performed. Haematoxylin and eosin staining and pH 2.5 Alcian blue staining with the hyaluronidase digestion test were performed on thin sections of 10% formalin or 10% neutral buffered formalin-fixed paraffin-embedded blocks, along with the assessment of the percentage and extent of the areas of GT.

GT cases were recorded at five levels, as described in a previous study. The grading was as follows: Max, diffuse marrow involvement; 3+, large foci; 2+, focal lesions of intermediate size; 1+, single microfocal involvement; and 0, no involvement[3]. The degree of hypocellular marrow with hyaluronidase-reactive pH 2.5 Alcian blue-positive deposits was defined as 2+ or higher and divided into the gelatinous marrow group and the no-change group. Watanabe's silver impregnation staining was performed in cases where fibrosis was suspected.

For the assessment of liver pathology, two pathologists separately observed non-neoplastic area of haematoxylin-eosin-stained microscopic specimen to determine if there were significant steatosis.

2. 5. 2 Immunohistochemical study

All immunohistochemical staining was performed on formalin-fixed paraffin-embedded blocks tissue sections using a Histofine simple stain AP (R) kit and simple stain MAX-PO (M), followed by a new fuchsin substrate solution kit and a diaminobenzide solution kit (Nichirei Bioscience, Tokyo, Japan). The following primary antibodies were used: stromal cell-derived factor 1/CXCL12 and rabbit monoclonal (immunohistochemistry-specific) clone D8G6H, 1:300 (Cell Signaling Technology, Danvers, MA, USA) ; CD10, mouse monoclonal, clone 56C6; CD68, mouse monoclonal; and clone PG-M1 ready-to-use (Nichirei Bioscience, Tokyo, Japan).

2. 6. Statistical analyses

The characteristics of patients with and without GT were compared using the chi-square test for categorical variables and the Mann–Whitney U test for continuous variables. Logistic regression analysis was used to assess the age- and sex-adjusted effect of each baseline characteristic: age, sex, malignancy, fatty or fibrous degeneration of the liver, and the presence of GT. Box and whiskers plots were used to evaluate median and interquartile ranges of each parameter. Statistical analyses were performed using R software version 4.2.1 (R Core Team, Vienna, Austria)[12].

III. Results

The baseline patient characteristics are shown in **Table 1.** Of the 104 participants enrolled, 18 (17%) were classified as having bone marrow GT. The histopathological findings and case distribution are shown in **Figure 2.** 15/18 (83%) patients had patchy GT lesions. Atrophy of fat cells and hypocellularity were observed within the GT area. There were two cases of bone marrow fibrosis coexisting with GT (**Figure 3**). In the complicated area, there was an increase in reticular cells, a mild increase in collagen fibres, and hyaluronidase digestion-reactive mucopolysaccharide deposition. Spindle cells in the fibrotic area were immunoreactive for CXCL12, CD10, and CD68.

CXCL12 is a chemokine that is widely expressed in a variety of stromal cells[13)-14)], reticulocytes expressing high levels of CXCL12 are called CXCL12-abundant reticular cells (CAR cells), which provide a haematopoietic environment for hematopoietic stromal cells and are themselves mesenchymal stem cells[15)-16)]. CAR cells were observed in various patterns, such as polygonal, stellate, spindle, and small round, and in the peri-adipose and peri-endothelial in normal (**Figure 4A**) and GT marrows (**Figure 4B, C, D**).

CD68 (PGM-1) is a specific marker for monocytes and histiocytes[17]. CD68 immunoreactive small round cells, mostly consistent with monocytes and stellate and spindle cells represented a part of the reticular cells and may have included CAR cells, and the giant cells were consistent with osteoclasts (**Figure 4E**).

CD10 is the enzyme primarily responsible for preadipocytes and adipocytes[18]. CD10 positivity was observed in the adipocytes. CD10 was also immunoreactive to spindle cells, consistent with some of the reticular cells and preadipocytes (**Figure 4F**).

CXCL12-CD68 co-expression in reticular cells was

Table 1 Baseline characteristics and comparison between the GT and non-GT groups

Item (unit)	N	GT group (N=18)	Non-GT group (N=86)	p-value[a]	Age-sex adjusted p-value
		n (%) or Median (IQR)			
Male sex	72	15 (83.3%)	57 (66.3%)	0.26	NA
Age (years)	104	76.0 [66.8–83.8]	71.5 [65.0–79.8]	0.2	NA
Malignancy	104	12 (66.7%)	46 (53.5%)	0.45	NA
Steatosis of the liver	103	9 (50.0%)	41 (48.2%)	1.00	NA
Fibrosis of the liver	103	7 (38.9%)	38 (44.7%)	0.85	NA
WBC count ($\times 10^9$/L)	104	9.26 [5.47–12.30]	11.92 [7.54–18.84]	0.15	0.10
Total neutrophil count ($\times 10^9$/L)	89	7.6 [4.10–9.60]	7.89 [3.63–14.68]	0.68	0.35
Total lymphocyte count ($\times 10^9$/L)	90	0.33 [0.23–0.74]	0.60 [0.34–0.89]	0.15	0.23
RBC count ($\times 10^{12}$/L)	104	3.08 [2.68–3.42]	3.12 [2.60–3.60]	0.85	0.91
Hemoglobin level (g/L)	104	92 [83.8–106.5]	95 [77.0–114.0]	0.99	0.68
Platelet count ($\times 10^9$/L)	104	154.0 [82–168.5]	117.5 [32–211.5]	0.31	0.84
Aspartate aminotransferase level (IU/L)	100	31.0 [21.8–64.3]	53.5 [25.0–133.5]	0.19	0.49
Alanine transaminase level (IU/L)	99	24.5 [10.5–51.3]	34.0 [15.5–65.5]	0.20	0.54
Alkaline phosphatase level (IU/L)	93	423 [217.3–1121.8]	379 [253.5–690.5]	0.59	0.039
Gamma-glutamyl transpeptidase level (IU/L)	94	94 [17.5–294.3]	68 [35.3–147.3]	0.84	0.36
Cholinesterase level (IU/L)	11	106 [86–126]	114 [100–179]	0.73	0.45
Total bilirubin level (mg/dL)	97	0.7 [0.6–2.6]	1.1 [0.6–2.7]	0.53	0.35
Total bilirubin level (μmol/L)		12.0 [10.3–44.5]	18.8 [10.3–46.1]		
TC level (mg/dL)	13	184 [119–249]	142 [118–156]	1.00	0.49
TC level (mmol/L)		4.76 [3.08–6.44]	3.67 [3.05–4.03]		
TG level (mg/dL)	10	48 [48–48]	92 [84–114]	0.20	1.00
TG level (mmol/L)		0.54 [0.54–0.54]	1.04 [0.95–1.29]		
Albumin level (g/L)	89	19 [18–24]	23 [19–28]	0.058	0.066
Total protein level (g/L)	67	48 [44–55]	55 [48–61]	0.095	0.19
Globulin level (g/L)[b]	67	28 [26–33]	29 [25–36]	0.89	0.93
Creatinine level (mg/dL)	98	0.75 [0.61–1.17]	1.42 [0.71–2.51]	0.047	0.085
Creatinine level (μmol/L)		66.3 [53.9–103]	126 [62.8–222]		
Creatinine level 3 weeks before death (mg/dL)	50	0.60 [0.49–0.74]	0.86 [0.64–1.24]	0.009	0.042
Creatinine level 3 weeks before death μmol/L)		53.0 [43.3–65.4]	76.0 [56.6–109]		
Uric acid level (mg/dL)	39	5.5 [4.0–8.3]	6.4 [4.5–8.56]	0.84	0.74
Uric acid level (μmol/L)		327 [238–494]	381 [268–509]		
CRP level (mg/dL)	99	7.3 [2.9–15.1]	6.1 [2.7–13.2]	0.94	0.52
CRP level (ug/L)		73000 [29000–151000]	61000 [27000–132000]		
Urine protein qualitative	33			0.44	0.51
−		0 (0%)	1 (3.3%)		
±		1 (33.3%)	6 (20%)		
1+		2 (66.7%)	15 (50%)		
2+		0 (0%)	5 (16.7%)		
3+		0 (0%)	3 (10%)		
Urine occult blood qualitative	33			0.42	0.56
−		1 (33.3%)	8 (26.7%)		
±		0 (0.0%)	3 (10.0%)		
1+		2 (66.7%)	6 (20.0%)		
2+		0 (0.0%)	11 (36.7%)		
3+		0 (0.0%)	2 (6.7%)		
BMI (kg/m^2)	90	18.6 [17.3–19.9]	21.9 [19.7–24.3]	<0.001	0.004
PNI (kg/m^2)	75	23.0 [19.6–27.4]	26.3 [22.0–33.4]	0.035	0.066
GNRI (kg/m^2)	76	66.8 [61.9–70.6]	75.9 [71.2–89.5]	0.002	0.007

GT, gelatinous transformation; IQR, interquartile range; WBC, white blood cell; RBC, red blood cell; TC, total cholesterol; TG, triglyceride; CRP, C-reactive protein; BMI, body mass index; PNI, prognostic nutritional index, GNRI, geriatric nutritional risk index.
* aMann–Whitney U tests were used for continuous variables; Chi-square tests were used for categorical variables. † bGlobulin: (Total protein)-(Albumin).

observed in the hematopoietic area, although the co-expressed stellate cells decreased in the GT area. Reticular cells with CXCL12-abundant long projections were consistent with CAR cells (**Figure 5**). These findings suggested that CAR cells, as mesenchymal stem cells, differentiate into fibroblasts, monocytes, macrophages, and adipocytes in the altered bone marrow, leading to hypocellularity.

A comparison between the GT and non-GT groups is presented in **Table 1.** GT was not significantly correlated to age or sex, nor presence or absence of malignancy. Both the GT and non-GT groups were anaemic; RBC (3.08 vs 3.12 10^{12}/L [male 4.35-5.55, female 3.86-4.92]), Haemoglobin (92 vs 95 g/L [male 137-168, female 116-148]), and had increased white blood cell counts and positive CRP levels (7.3 vs 6.1 mg/dL, 73000 vs 61000 μg/L), but there were no significant differences.

Fatty degeneration of the liver was observed in nearly

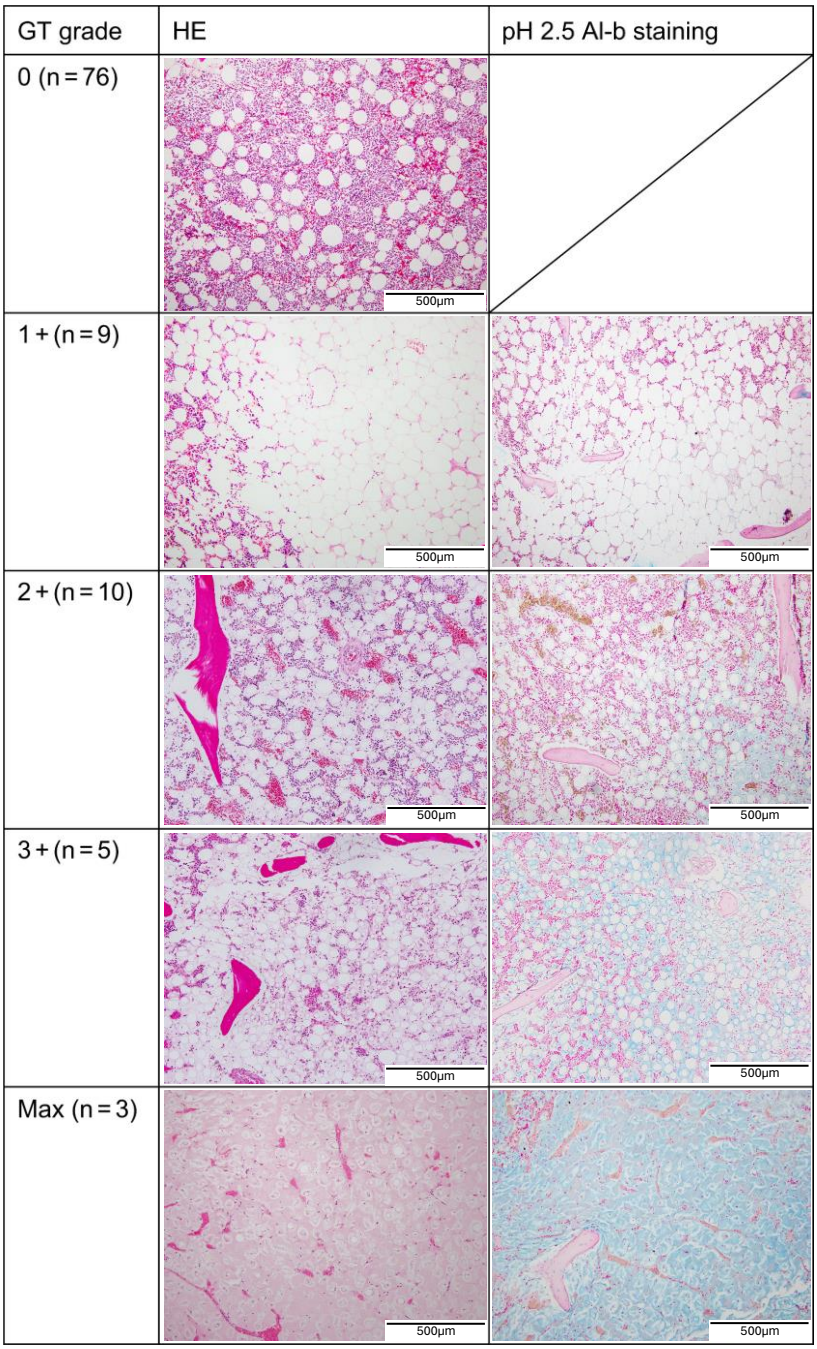

Figure 2 Histological grading of gelatinous transformation (scale bar=200 μm).
GT areas are patchily distributed in most cases. HE, haematoxylin-eosin staining; Al-b, pH 2.5 Alcian blue staining; GT, gelatinous transformation.

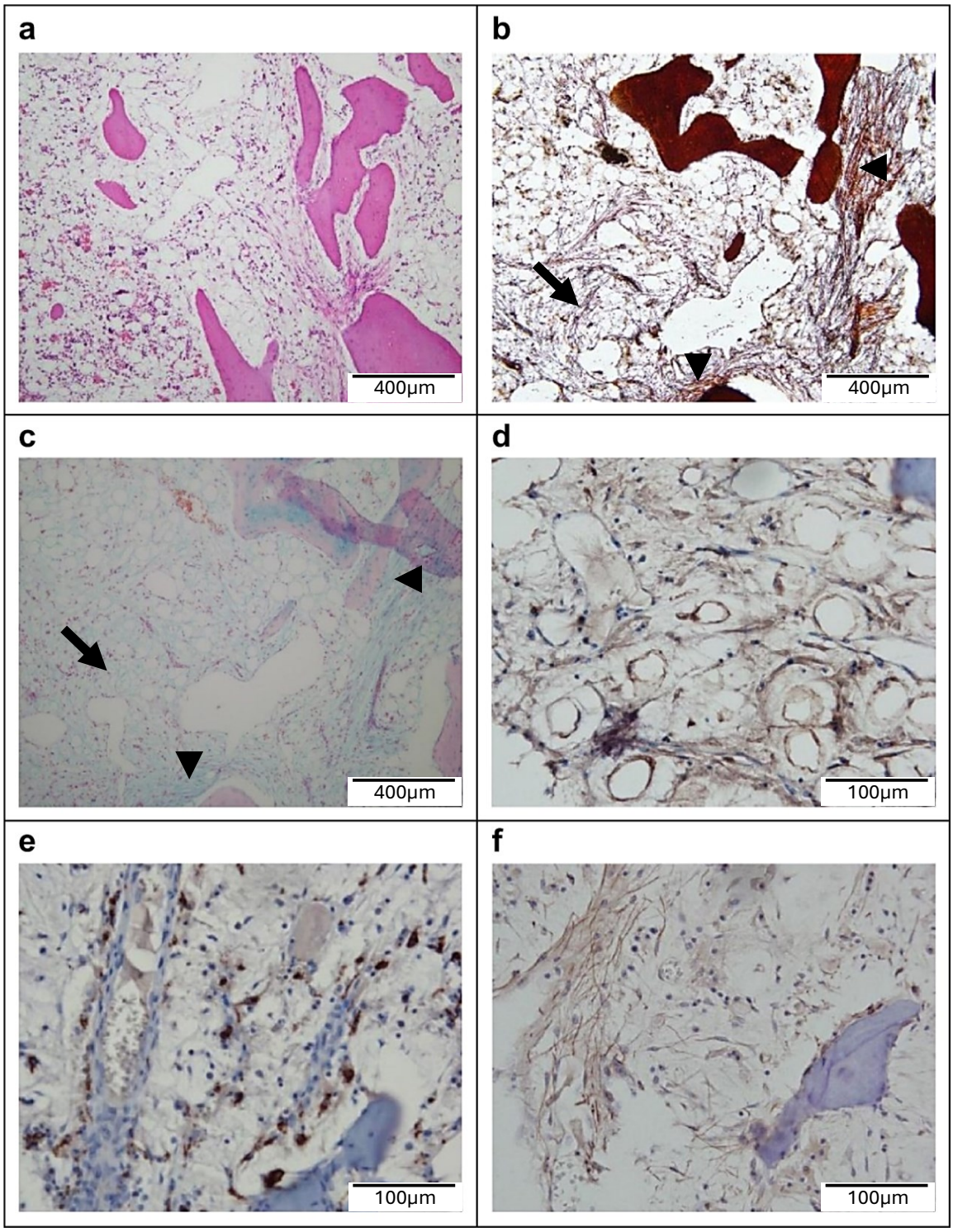

Figure 3 Microscopic findings of GT with fibrosis cases (A: scale bar=100 μm, B−F: scale bar=50 μm).
A. Haematoxylin-eosin staining. Bone and fibrous materials are increased. B. Silver impregnation staining. Brown-black reticular fibres (arrows) and brown-red collagen fibres (arrowheads) are increased. C. pH 2.5 Alcian blue staining. Blue colour is observed in both the GT and fibrotic area. These are both-hyaluronidase reactive. B, C. Serial sections. Bone tissue is displaced by sectioning artifacts. D. CD10-immunohistochemistry (IHC). A few spindle cells and fat cells show positivity. E. CD68-IHC. Monocytes, macrophages, periosteal giant cells, and some spindle cells are immunoreactive for CD68. F. CXCL12-IHC. The fibre-like projection of some spindle cells in fibrosis is positive. CXCL12, C-X-C motif chemokine ligand 12; GT, gelatinous transformation.

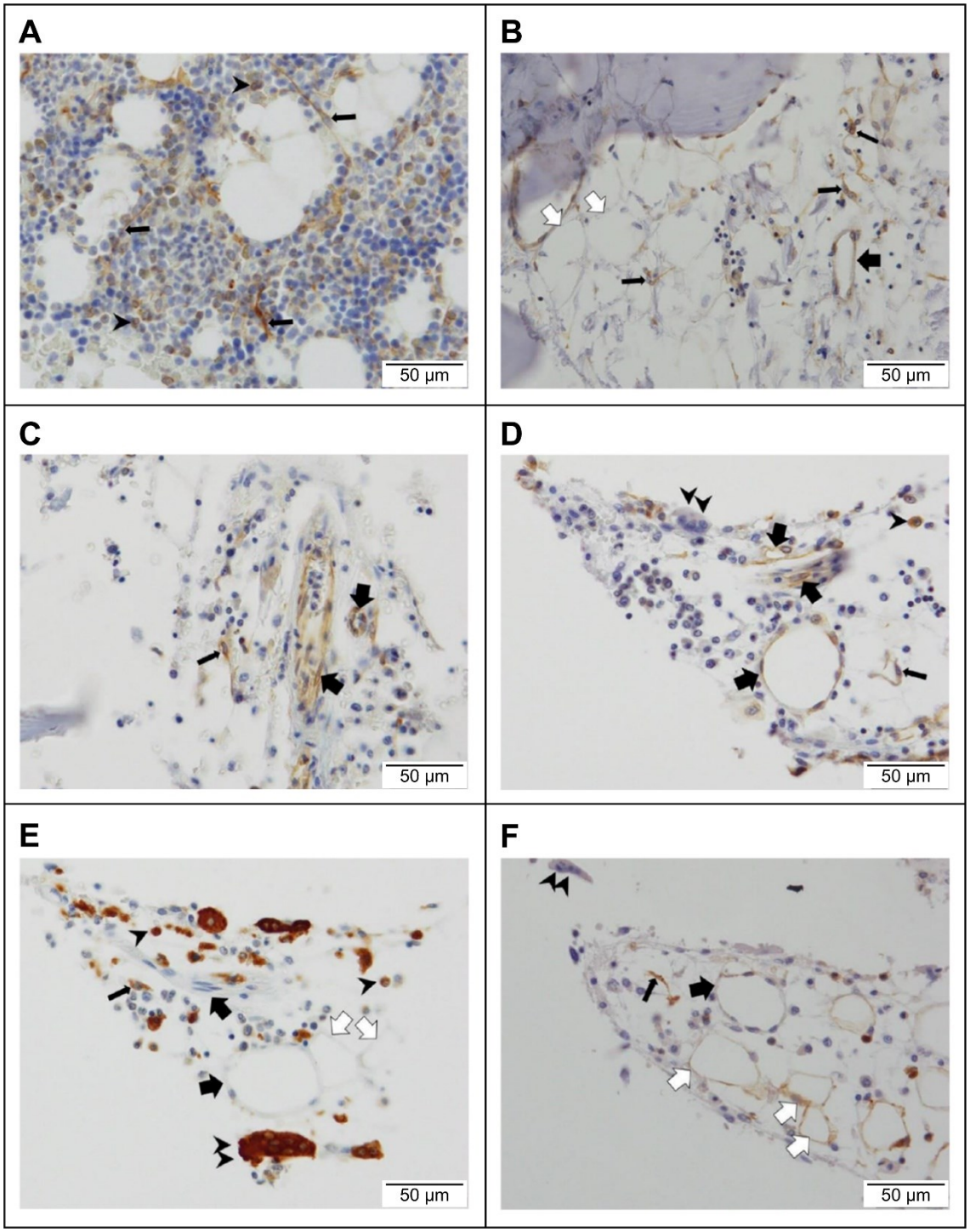

Figure 4 Immunohistochemical findings of GT marrow (scale bar=50 μm).
A: CXCL12-immunohistochemistry (IHC) in normal control. CXCL12 immunoreactive small round cells (arrowheads) and stellate cells are seen. Long projections of stellate cells among hematopoietic cells are strongly positive (arrows). These may be CAR cells. B–D: CXCL12- IHC in the GT marrow. B, C: CXCL12 positivity is observed in spindle cells (small black arrows), peri-adipose cells (white arrows), and peri-endothelial (black arrows). D: CXCL12 positivity is observed in small round cells (arrowhead), spindle cells (small black arrow), and peri-endothelial area (black arrows), but not for giant cells (double arrowheads). E: CD68-IHC in the GT marrow. Small round cells (arrowheads), spindle cells (small black arrow), and giant cells (double arrowheads) were immunoreactive. The peri-endothelial area (black arrows) and adipose cells (white arrows) were not reactive for CD68. F: CD10-IHC in the GT marrow. Fat cells (white arrows) and spindle cells (small black arrow) are immunoreactive but are not reactive for the peri-endothelial area (black arrows), giant cells (double arrowhead). D–F are complete serial sections. Bone tissue around the bone marrow tissue is off-screen due to sectioning artifacts. CXCL12, C-X-C motif chemokine ligand 12; CAR cells, C-X-C motif chemokine ligand 12-abundant reticular cells; GT, gelatinous transformation.

half of the patients in both groups, seemed to suggest steatohepatitis due to nutritional disorders, but there was no significant difference between the two groups. In both groups, Gamma-glutamyl transpeptidase level was above the reference range [male13-64, female 9-32], but median total bilirubin remained in the reference standard range [0.4-1.5mg/dL, 6.8-26.3μmol/L]. Median ALT, suggestive of hepatocellular damage, was slightly higher than the reference range [24.5 vs 34.0 IU/L male10-42, female 7-23 IU/L], reflecting organ damage immediately before death, but was lower in the GT group than in the non-GT group, with no significant difference between the two groups [24.5 vs 34.0 IU/L].

Median serum creatinine (sCr) in the non-GT group was high (1.42 mg/dL [male 0.66-1.06, female 0.46-0.79]; 66.3 vs. 126 μmol/L [male 72.7-109.1, female 54.5-81.8]). reflects various renal dysfunctions immediately prior to death, while median sCr in the GT group was in

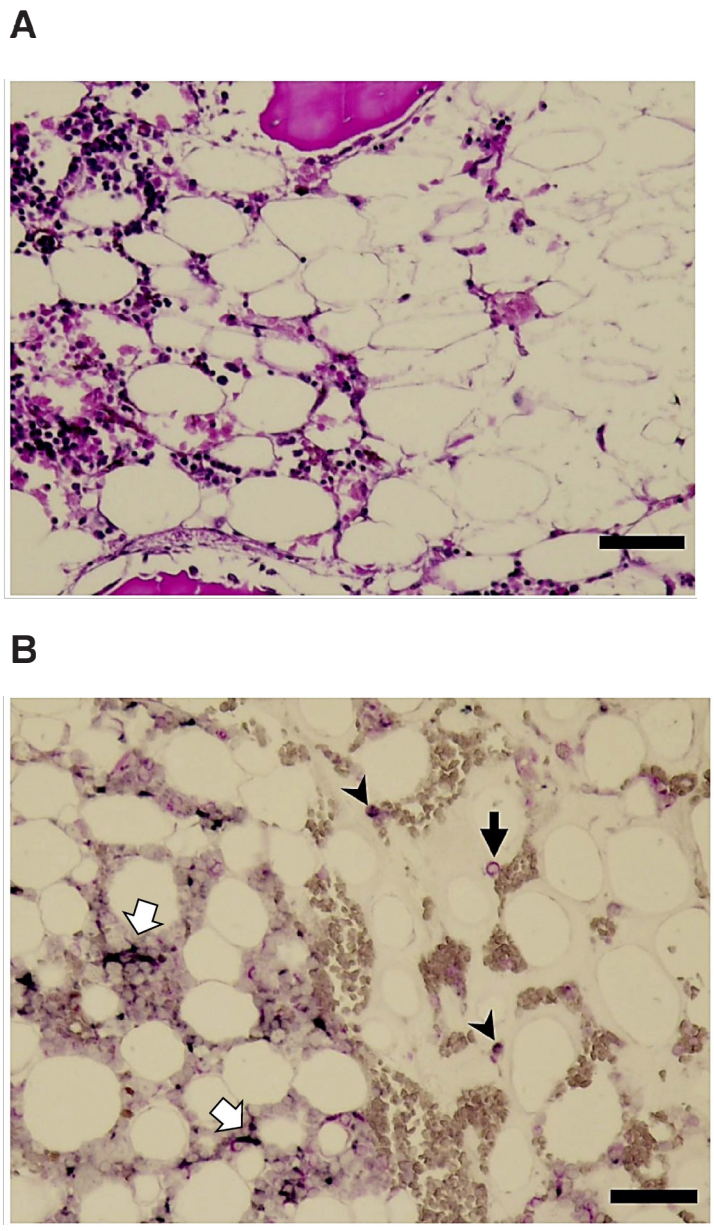

Figure 5 Double-immunostaining results for CXCL12 and CD68 in GT (scale bar=100 μm).
A: Haematoxylin-eosin staining of GT marrow. The left half is the normocellular area, and right half is the patchy GT area. B. CXCL12 (red) CD68 (blue black) double immunostaining in the GT marrow. Stellate reticular cells that express CXCL12 in long projections and CD68 in cytoplasm (white arrows) are seen in the normocellular area. Reticular cells have shortened CXCL12-positive projections (arrowheads), and CXCL12-positive small round cells (black arrow) are observed in the GT area. CXCL12, C-X-C motif chemokine ligand 12; GT, gelatinous transformation.

the reference range (0.75 mg/dL, 66.3 μmol/L). The GT group also had significantly lower sCr levels than the non-GT group (p=0.047). The sCr level 3 weeks before death are significantly lower in GT group, after adjusting the age- and sex (p=0.042).

Both groups had low median albumin level (19 vs. 23 g/L [41-51]) and The GT group tended to have lower albumin than the non-GT group (p=0.066). Similarly, both groups had lower BMI (18.6 vs. 21.9 kg/m^2 [22.6-27.5]), and GNRI (66.8 vs.75.9 kg/m^2), but the GT group had significantly lower BMI and GNRI than the non-GT group (p<0.001 and p=0.002, respectively). The exact data are shown in **Figure 6**.

IV. Discussion

We investigated GT marrow at autopsy and found that

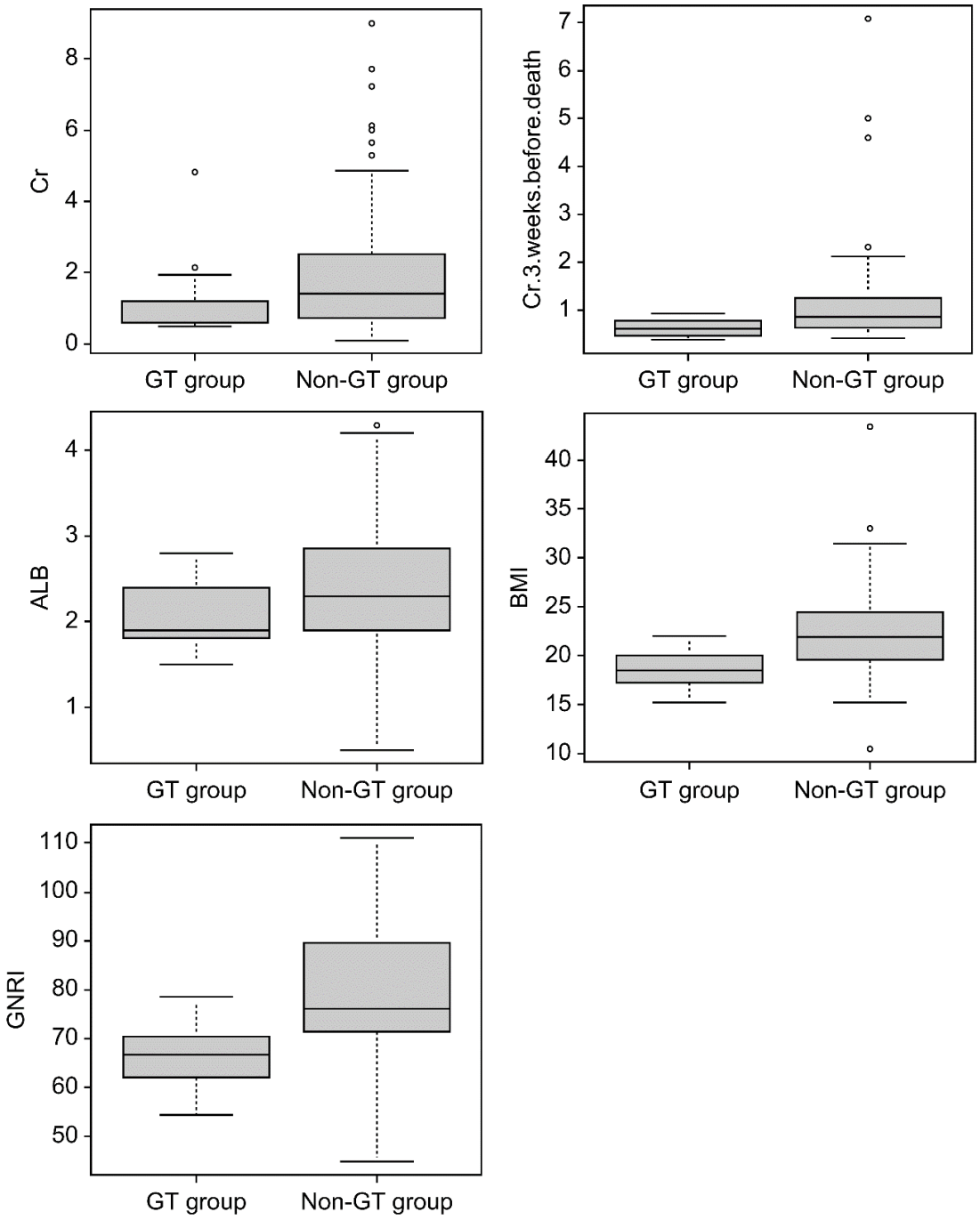

Figure 6 Comparison of each parameter between GT and non-GT groups.
GT, gelatinous transformation; BMI, body mass index; GNRI, geriatric nutritional risk index; Cr, creatinine; ALB, albumin.

the GT area had different reticular cell conditions. And our analysis of clinico-laboratory data of GT and non-GT patients. As previously hypothesized, we confirmed a strong association with malnutrition; however, unlike previous hypotheses [1)-6)], there was weak association with anaemia. Furthermore, we reported interesting phenomenon that the sCr of the GT patients remained in the reference range, even just before death.

We speculated that the significantly lower sCr levels had been observed in the GT group from 3 weeks prior form death were related to the presence of muscle loss. Recently low sCr "on admission" has been theorized to be related to sarcopenia when other causes can be ruled out [19)-24)]. Our series do not have patients with fluid excess condition, myoneuropathy, paralysis or limb amputation. Liver dysfunction was negative in the data analysis, suggesting muscle reduction as a possible cause.

Nutrition indicators, both groups had low median BMI, but the GT group had a median value below 2.0 kg/m^2, which is a poor prognosis for life [25)-26)]. Protein-energy malnutrition (PEM) is the condition of lack of energy due to the deficiency of all the macronutrients and many micronutrients [27)]. in recent years, PEM is known as the main cause of sarcopenia; defined as a progressive and generalized skeletal muscle disorder involving the accelerated loss of muscle and its function [28)-29)]. In children, marasmic kwashiorkor phenotypes are also present [26) 30)-31)], but in adults, which are more common in nutritional disorders in developed countries, there are two major types of PEM: marasmus/cachexia, and kwashiorkor/protein-calorie malnutrition (PCM) [27)]. Marasmus/cachexia is balanced malnutrition caused by long-standing starvation or chronic systemic inflammation. The prognosis for marasmus/cachexia is relatively good, although it involves substantial loss of body mass, with body weight less than 80% of the standard for height [26)-27)]. Thus, low BMI in our GT group represents marasmus/cachexia. In contrast, kwashiorkor/PCM is caused by loss of relative protein intake. In 1933, Williams reported kwashiorkor in children in the Gold Coast of West Africa. Kwashiorkor fatality was as high as 90% and fatty change of the liver was observed in autopsy [27) 30)-31)]. In developed countries, kwashiorkor/PCM may occur within weeks of subsequent acute life-threatening illnesses, such as trauma and sepsis. The patients look well-nourished because of systemic oedema; however, their blood shows hypoalbuminemia and lymphocytopenia. Under stressed conditions, patients with kwashiorkor/PCM show hypermetabolism with high cytokine levels, such as tumour necrosis factor alpha, interleukin-1, and interleukin-6 and high stress hormone levels, such as catecholamine, glucagon, and cortisol, which leads to proteolysis and absolute fat catabolism, poor wound healing, and impaired host deficiency [26)]. Considering the significantly lower albumin and higher CRP levels in the GT group, it is likely that the GT have a severe condition of anabolic failure as seen in kwashiorkor/PCM.

In the GT group, except in a small number of maximal cases, the bone marrow hypocellularity associated with GT was patchily distributed and haematopoietic area remained. We consider this histological feature reflects the low association between GT and anaemia. In the GT area, various morphologies of CXCL-12 positive mesenchymal cells co-expressed multiple mesenchymal molecules, such as CD10 or CD68 and CXCL12-abundant projections were less observed. We estimate this histological finding implies CAR cells differentiation and haemopoietic cell depletion [32)]. Like GT, Mucopolysaccharide accumulation in deep connective tissue is often observed in myxoedema, a thyroid hormone dysregulation [33) 34)]. However, the mechanisms and histology of the dysthyroid status have not been adequately reported. The trends in clinical data that were significant in the GT group patients in this study appear to have much in common with thyroid hormone abnormalities, particularly the low T3 syndrome (also known as non-thyroidal disease syndrome).[35)] It would be beneficial to consider the common features of GT with the low T3 syndrome.

A limitation of this study is that the required sample size was not met. The study design, a retrospective observational study, resulted in many missing items like hormone test values. Also, we could not obtain good staining results due to damage from specimen decalcification. we should have performed immunostaining for many bone marrow mesenchymal markers such as leptin, CD163, and adipophilin, but we could not obtain good staining results due to damage from specimen decalcification.

In conclusion, 17% of autopsy adult cases had overt GT; 83% had patchy progression. Mesenchymal cells in the GT region co-expressed multiple molecules. Bone marrow GT was associated with low BMI, GNRI, and low sCr level. These results suggest that bone marrow GT is associated with PEM with muscle loss, but not with anaemia.

Acknowledgment

We would like to thank Professor Ayumi Shintani of Osaka Metropolitan University for organizing the Statistics for Research Skills seminar through the Awa Support Centre.

Funding

None.

Authorship Contributions

ST, MY, and TK collected laboratory data and performed statistical analysis; MY supervised the study and analysed bone marrow histopathology; MIS reviewed and interpreted nutritional indices; SS and KT analysed liver histopathology; and MK, ST, and SW prepared pathology specimens. All authors read and approved the final paper.

Disclosure of Conflict of Interest

The authors declare no conflict of interest.

References

1) Michael P. Gelatinous degeneration of the bone marrow. J Pathol 1930; 33 (3): 533-8.
2) Mills SE. Histology for pathologists. 5th ed. Wolters Kluwer; 2019.
3) Böhm J. Gelatinous transformation of the bone marrow: the spectrum of underlying diseases. Am J Surg Pathol 2000; 24 (1): 56-65.
4) Seaman JP, Kjeldsberg CR, Linker A. Gelatinous transformation of the bone marrow. Hum Pathol 1978; 9 (6): 685-92.
5) Shergill KK, Shergill GS, Pillai HJ. Gelatinous transformation of bone marrow: rare or underdiagnosed? Autops Case Rep 2017; 7 (4): 8-17.
6) Sen R, Singh S, Singh H, et al. Clinical profile in gelatinous bone marrow transformation. J Assoc Physicians India 2003; 51: 585-8.
7) Ichihara K, Yamamoto Y, Hotta T, et al. Collaborative derivation of reference intervals for major clinical laboratory tests in Japan. Ann Clin Biochem 2016; 53 (Pt 3): 347-56.
8) Nuttall FQ. Body mass index: obesity, BMI, and health: a critical review. Nutr Today 2015; 50 (3): 117-28.
9) Onodera T, Goseki N, Kosaki G. Prognostic nutritional index in gastrointestinal surgery of malnourished cancer patients. Nihon Geka Gakkai Zasshi 1984; 85 (9): 1001-5.
10) Bouillanne O, Morineau G, Dupont C, et al. Geriatric Nutritional Risk Index: a new index for evaluating at-risk elderly medical patients. Am J Clin Nutr 2005; 82 (4): 777-83.
11) Zheng W, McLerran DF, Rolland B. et al. Association between Body-Mass Index and Risk of Death in More Than 1 Million Asians. N Engl J Med 2011; 364 (8):719-29.
12) R: A Language and Environment for Statistical Computing [Internet]; 2022. [cited 2022.12.1]. Available from: https://www.R-project.org/. Vienna: R Core Team.
13) Nagasawa T, Hirota S, Tachibana K, et al. Defects of B-cell lymphopoiesis and bone-marrow myelopoiesis in mice lacking the CXC chemokine PBSF/SDF-1. Nature 1996; 382 (6592): 635-8.
14) Sugiyama T, Kohara H, Noda M, et al. Maintenance of the hematopoietic stem cell pool by CXCL12-CXCR4 chemokine signaling in bone marrow stromal cell niches. Immunity 2006; 25 (6): 977-88.
15) Prasad P, Cancelas JA. From Marrow to Bone and Fat: Exploring the Multifaceted Roles of Leptin Receptor Positive Bone Marrow Mesenchymal Stromal Cells. Cells 2024; 13 (11): 910.
16) Omatsu Y, Aiba S, Maeta T, et al. Runx1 and Runx2 inhibit fibrotic conversion of cellular niches for hematopoietic stem cells. Nat commu 2022; 13 (1): 2654.
17) Khoury JD, Solary E, Abla O, et al. The 5th edition of the World Health Organization Classification of Haematolymphoid Tumours: myeloid and Histiocytic/Dendritic Neoplasms. Leukemia 2022; 36 (7): 1703-19.
18) Ding L, Vezzani B, Khan N, et al. CD10 expression identifies a subset of human perivascular progenitor cells with high proliferation and calcification potentials. Stem Cells 2020; 38 (2): 261-75.
19) Lien YHH. Looking for sarcopenia biomarkers. Am J Med 2017; 130 (5): 502-3.
20) Park J, Mehrotra R, Rhee CM, et al. Serum creatinine level, a surrogate of muscle mass, predicts mortality in peritoneal dialysis patients. Nephrol Dial Transplant 2013; 28 (8): 2146-55.
21) Schutte JE, Longhurst JC, Gaffney FA, et al. Total plasma creatinine: an accurate measure of total striated muscle mass. J Appl Physiol Respir Environ Exerc Physiol 1981; 51 (3): 762-6.
22) Thongprayoon C, Cheungpasitporn W, Kashani K. Serum creatinine level, a surrogate of muscle mass, predicts mortality in critically ill patients. J Thorac Dis 2016; 8 (5): E305-11.
23) Chen LK, Liu LK, Woo J, et al. Sarcopenia in Asia: consensus report of the Asian Working Group for Sarcopenia. J Am Med Dir Assoc 2014; 15 (2): 95-101.
24) Cruz-Jentoft AJ, Baehens JP, Bauer JM, et al. Sarcopenia: European consensus on definition and diagnosis: Report of the European working group on sarcopenia in older People. Age Ageing 2010; 39 (4): 412-23.
25) Nuttall FQ. Body Mass Index: Obesity, BMI, and Health: A Critical Review. Nutr Today. 2015; 50 (3): 117-28.
26) Grover Z, Ee LC. Protein energy malnutrition. Pediatr Clin North Am 2009, 56 (5): 1055-68.
27) Heimburger DC. Malnutrition and nutritional assessment. Harrison's principles of internal medicine, 18th ed. McGraw-Hill Professional 2011; 605-11.
28) Cruz-Jentoft AJ, Sayer AA. Sarcopenia. Lancet 2019; 393 (10191): 2636-46.

29) Anker SD, Morley JE, von Haehling S. Welcome to the ICD-10 code for sarcopenia. J Cachexia Sarcopenia Muscle 2016; 7 (5) : 512-4.
30) Williams CD. A nutritional disease of childhood associated with a maize diet. Arch Dis Child 1933; 8 (48) : 423-33.
31) Williams CD, Oxon BM, BRCP, et al. Kwashiorkor, A nutritional disease of children associated with a maize diet. Lancet 1935; 226 (5855) : 1151-2.
32) Omatsu Y, Nagasawa T. Identification of microenvironmental niches for hematopoietic stem cells and lymphoid progenitors–bone marrow fibroblastic reticular cells with salient features. Int Immunol 2021; 33 (12) : 821-6.
33) Elshimy G, Chippa V, Correa R. Myxedema. StatPearls [Internet]. Treasure Island (FL) : StatPearls Publishing; 2024. Last Update: August 14, 2023.
34) Rongioletti F, Rebora A. Cutaneous mucinoses: microscopic criteria for diagnosis. Am J Dermatopathol. 2001; 23 (3) : 257-67.
35) Fliers E, Bianco AC, Langouche L, et al. Thyroid function in critically ill patients. Lancet Diabetes Endocrinol, 2015; 3 (10) : 816-25.